

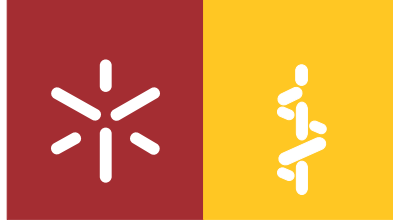


Universidade do Minho
Escola de Medicina

Caroline Isabel Borges Pereira

**Epithelial and vascular compartments
modulation by tissue macrophages during
lung development**

**Modelação do desenvolvimento pulmonar
epitelial e vascular pelos macrófagos
tecidulares**



Universidade do Minho
Escola de Medicina

Caroline Isabel Borges Pereira

**Epithelial and vascular compartments
modulation by tissue macrophages during
lung development**

**Modelação do desenvolvimento pulmonar
epitelial e vascular pelos macrófagos
tecidulares**

Dissertação de Mestrado
Mestrado em Ciências da Saúde

Trabalho efetuado sob a orientação da
Doutora Sandra Maria Araújo da Costa

setembro de 2017

DECLARAÇÃO

Nome: Caroline Isabel Borges Pereira

Endereço eletrónico: carolinebp1994@gmail.com

Bilhete de Identidade/Cartão do Cidadão: 14542283

Título da dissertação: Epithelial and vascular compartments modulation by tissue macrophages during lung development

Orientadora:

Doutora Sandra Maria Araújo da Costa

Ano de conclusão: 2017

Mestrado em Ciências da Saúde

DE ACORDO COM A LEGISLAÇÃO EM VIGOR, NÃO É PERMITIDA A REPRODUÇÃO DE QUALQUER PARTE DESTA DISSERTAÇÃO

Universidade do Minho, 20/09/2017

Assinatura:

Caroline Isabel Borges Pereira

Aos meus pais, ao meu irmão, à Márcia e ao Pedro

Agradecimentos

Ao fim destes dois anos, guardo em mim pequenas recordações de todas as pessoas que me acompanharam nesta longa viagem de conhecimento não só científico, mas também da vida. Guardo cada pedacinho dentro do meu coração e expresso aqui os meus profundos agradecimentos pela paciência, disponibilidade, alegria, animação e ajuda prestada ao longo desta caminhada.

Em primeiro lugar, gostaria de agradecer à Doutora Sandra Costa pela oportunidade de experienciar um ano de árduo trabalho laboratorial, de muita experiência científica e profissional, pela partilha de conhecimento e incentivo à procura de novas respostas, pela forma alegre e responsável com a qual me propunha novos desafios, pelos debates científicos acerca dos resultados obtidos, pelos sonhos de novos projetos e novas ambições, pelas propostas futuras de um trabalho árduo mas com uma recompensa final incalculável. Um grande obrigada por me ter feito crescer ao longo deste tempo, não só a nível profissional, mas também a nível pessoal.

Em segundo lugar, agradecer a toda a equipa laboratorial: Ana Freitas, Catarina Matos e Sofia Libório. Um grande obrigado por toda a ajuda na realização desta tese de mestrado, e um grande obrigado por todo o apoio prestado e por esta amizade que guardo para toda a minha vida. Sem vocês, esta tese não estaria aqui, obrigada!

Um especial obrigado à pessoa que mais me aturou ao longo deste ano de tese. Obrigada pela companhia, pelos almoços e jantares feitos pela tua mãe, obrigada pelas risas e os choros partilhados, obrigada pelas brincadeiras e pelos desabafos. Tens um lugarzinho muito especial aqui dentro Sofia Libório do Facebook!

Gostaria de agradecer toda a amabilidade, simpatia, ajuda e animação demonstrada pelos meus colegas dos laboratórios I1.02 e I1.03.

Aos meus colegas de mestrado, um profundo obrigado pelo ano maravilhoso que vivemos e por todas as brincadeiras, as saídas, os almoços, os lanches, as ajudas entre os grupos de laboratório, a troca de informações e de conhecimento, os desabafos e tudo o que por nós foi vivenciado. Um grande obrigado!

Aos meus melhores amigos Márcia Vaz, Vitor Ferreira, Ana Lima, Diogo Silva, Sofia Libório, Tiago Rodrigues, Ivo Barreira, Joana Santos e Ana Pires por todo o apoio prestado, não só ao longo destes dois anos, mas de toda uma vida. Obrigada!

Um especial agradecimento à Marta Pojo e ao Filipe Pinto, pois foi graças a todos os vossos conselhos que eu cheguei aqui. Obrigada!

Um especial e carinhoso agradecimento ao Pedro, um dos grandes pilares da minha vida e a pessoa que mais me apoia em qualquer tipo de situação. Obrigada por estes anos maravilhosos ao teu lado. Desejo-te as maiores felicidades do mundo, e espero estar ao teu lado para as vivenciar contigo. Esta vitória é nossa!

E por fim, aos meus pais o MAIOR OBRIGADO, pois sem eles a minha vida não teria este maravilhoso sentido, espero deixar-vos bastante orgulhosa no final desta minha etapa. E que muitas mais etapas venham e que as possamos celebrar todos juntos. Um ENORME obrigado ao meu irmão Luís por todas as demonstrações de afeto em todos os momentos da minha vida. És o meu orgulho Luís! Amo-vos, muito!

O trabalho apresentado nesta dissertação de tese foi realizado no Instituto de Investigação em Ciências da Vida e Saúde (ICVS), Universidade do Minho.

O financiamento para a realização deste projeto provém dos fundos do Programa Operacional Regional do Norte (NORTE 2020), sobre o Acordo de Parceria PORTUGAL 2020, através do Fundo Europeu de Desenvolvimento Regional (FEDER). O financiamento da FEDER advém também do Programa Operacional Fatores de Competitividade – COMPETE, e dos fundos nacionais através da Fundação para a Ciência e Tecnologia sobre POCI-01-0145-FEDER-007038; e sobre o projeto NORTE-01-0145-FEDER-000013.



Fundação para a Ciência e a Tecnologia
MINISTÉRIO DA CIÊNCIA, TECNOLOGIA E ENSINO SUPERIOR



Abstract

Preterm birth is one of the causes of mortality and morbidity in childhood mainly due to lung immaturity. Glucocorticoids therapy is administered to promote lung maturation. However, recent studies showed that glucocorticoids promote several side effects, as respiratory and neurological impairments during child and mostly adulthood. The search for new therapeutic approaches is necessary to improve life quality of these individuals. Recently, tissue macrophages were described as fundamental effectors in the modulation of several organs development, mainly in processes such as branching morphogenesis and vasculature formation. In lung, it is known that they are present since the beginning of lung embryonic stage (embryonic day (E) 9.5). However, their function throughout lung development is unknown. Using a macrophage-deficiency mice model (colony stimulating factor-1 receptor knockout (*Csf1r*^{-/-}) mice) team unpublished data showed impairments in lung morphology, with decreased airspaces and increased number of mesenchyme-like cells at fetal and postnatal saccular lung developmental stage. This stage is mainly characterized by specification of the terminal sacs, and alveolar and vasculature differentiation.

Accordingly, we hypothesized that tissue macrophages are involved in regulation of distal epithelium and vasculature differentiation during the saccular stage. In order to test this, we investigated lung epithelial markers and vascular mediators' transcripts and proteins expression in lung tissues from fetal and newborns *Csf1r*^{-/-} mice at saccular stage.

Transcripts relative expression of distal epithelium markers evidenced a disequilibrium at alveolar differentiation. Protein expression analyses of Sp-c (ATII cell marker) and Aqp5 (ATI cell marker) demonstrated a reduction in alveolar differentiation in *Csf1r*^{-/-} mice at saccular stage. Since the epithelial-endothelial crosstalk is crucial to a normal lung development, vasculature was also investigated. Analysis of some vascular mediators showed an unbalance at transcript expression levels in *Csf1r*^{-/-} mice lungs. Additionally, protein expression evaluation of two specific endothelial markers showed impairments in vasculature formation in most of *Csf1r*^{-/-} lungs. However, vascular defects emerged later in development compared with the alveolar disruption.

In summary, our data demonstrate the influence of fetal tissue macrophages in the modulation of alveolar epithelium differentiation, with consequently effects on vasculature, probably by the secretion and/or induction of specific mediators. New therapeutic approaches may rise from these tissue macrophages mediators to accelerate lung maturation.

Resumo

O nascimento prematuro é uma das principais causas de mortalidade e morbidade durante a idade infantil devido à imaturidade pulmonar. A administração de glucocorticoides como terapia promove a maturação pulmonar. No entanto, estudos recentes demonstram que a sua administração promove diversos feitos adversos, nomeadamente problemas respiratórios e neurológicos durante uma idade infantil e principalmente na idade adulta. A procura de novas abordagens terapêuticas é necessária de modo a melhorar a qualidade de vida destes indivíduos. Recentemente, os macrófagos tecidulares foram descritos como células fundamentais na modulação do desenvolvimento de vários órgãos, principalmente nos processos de ramificação morfogénica e na formação da vasculatura. No pulmão sabe-se que estes estão presentes desde o início da fase embrionária (dia embrionário (E) 9.5). No entanto, a sua função ao longo do desenvolvimento pulmonar é desconhecida. Utilizando um modelo de ratinho deficiente em macrófagos tecidulares (*colony stimulating factor-1 receptor knockout (Csf1r^{-/-})*), dados não publicados da equipa demonstram malformações na morfologia pulmonar, com um decréscimo nos espaços aéreos e um aumento do número de células do tipo mesenquimatoso durante o período fetal e pós-natal da fase sacular do desenvolvimento pulmonar. Esta fase é maioritariamente caracterizada pela especificação dos sacos terminais, e diferenciação dos alvéolos e da vasculatura.

Portanto, a nossa hipótese é que os macrófagos tecidulares estão envolvidos na regulação da diferenciação do epitélio distal e da vasculatura durante a fase sacular. De modo a testar esta hipótese, nós estudámos a expressão dos transcritos de marcadores do epitélio e de mediadores da vasculatura e a sua expressão proteica em pulmões provenientes de fetos e recém-nascidos *Csf1r^{-/-}* na fase sacular.

A expressão relativa dos transcritos de moléculas relacionadas com o epitélio distal evidenciou um desequilíbrio na diferenciação alveolar. A expressão proteica da proteína surfactante C (marcador de células alveolares do tipo II) e da aquaporina-5 (marcador de células alveolares do tipo I) demonstraram uma redução na diferenciação alveolar nos ratinhos *Csf1r^{-/-}* na fase sacular. Sendo a interação epitélio-endotélio crucial para um normal desenvolvimento pulmonar, a vasculatura foi também estudada. A análise de alguns mediadores vasculares demonstrou um desequilíbrio nos níveis de expressão destes transcritos nos pulmões dos ratinhos *Csf1r^{-/-}*. Adicionalmente, a expressão proteica de dois marcadores endoteliais demonstrou deficiências na formação vascular

na maioria dos pulmões de ratinhos *Csf1r*^{-/-}. No entanto, este distúrbio na formação da vasculatura foi evidente apenas mais tarde no desenvolvimento em comparação com os defeitos epiteliais alveolares.

Em sumário, os nossos dados demonstram a influência dos macrófagos tecidulares na modulação da diferenciação do epitélio alveolar, com consequentes efeitos na vasculatura, provavelmente devido à secreção e/ou indução de mediadores específicos. Novas abordagens terapêuticas poderão surgir dos mediadores produzidos pelos macrófagos tecidulares para acelerar a maturação pulmonar.

Table of contents

Agradecimentos	v
Abstract.....	vii
Resumo.....	ix
Abbreviation List.....	xiii
Figure List.....	xvii
1. INTRODUCTION	1
1.1 Lung development	3
1.1.1 Airways unit development.....	5
1.1.2 Respiratory unit development.....	7
1.2 Tissue macrophages during organs development	9
1.2.1. Tissue macrophages and organogenesis.....	9
1.2.2. Tissue macrophages and lung development.....	11
2.AIMS	13
3.MATERIALS AND METHODS.....	17
3.1 Animals, Ethics and Tissue collection	19
3.2 DNA extraction and Genotyping PCR.....	19
3.3 Reverse transcriptase -quantitative PCR.....	20
3.3.1 RNA extraction.....	20
3.3.2 cDNA conversion	20
3.3.3 qPCR.....	20
3.4 Immunofluorescence	21
3.4.1 Immunofluorescence of alveolar epithelial cells markers	21
3.4.2 Immunofluorescence of endothelial cells markers.....	22
3.4.3 Confocal microscopy and quantitative analysis	22
3.5 Tissue culture.....	23
3.5.1 Lung slices culture.....	23
3.5.2 Tissue processing, microscopy and cell death analysis.....	24
3.6 Statistical analysis	24
4.RESULTS	25
4.1 Tissue macrophages involvement in alveolar differentiation	27
4.2 Tissue macrophages modulation of bronchiole differentiation	35
4.3 Impact of tissue macrophages in lung vasculature formation	38
5.DISCUSSION.....	47

6.CONCLUSIONS	55
7.REFERENCES.....	59
8.SUPPLEMENTARY INFORMATION	69

Abbreviation List

A

Abca3	ATP binding cassette subfamily A member 3
Ang-1	Angiopoietin-1
Ang-2	Angiopoietin-2
Aqp5	Aquaporin-5
AT1	Alveolar cells type I
AT2	Alveolar cells type II

B

Bmp	Bone morphogenetic protein
bp	Base pair
BSA	Bovine serum albumin

C

Calca	Calcitonin
Cd31	Platelet endothelial cell adhesion molecule
cDNA	Complementary DNA
CO ₂	Carbon dioxide
CPP	Cardiopulmonary mesoderm progenitors
Csf1	Colony stimulating factor-1
Csf1r	Colony stimulating factor-1 receptor
Csf2	Colony stimulating factor-2

D

DAPI	4',6-Diamidine-2'-phenylindole dihydrochloride
DMEM	Dulbecco's Modified Eagle Medium
DMEM/F12	Dulbecco's Modified Eagle Medium: Nutrient Mixture F-12
DNA	Deoxyribonucleic Acid

E

E	Embryonic Day
E-cad	E-cadherin
EDTA	Ethylenediamine tetraacetic acid
EGF-M7	Adhesion G protein-coupled receptor E1
EGFP	Enhanced green fluorescence protein

F

F4/80 Cell surface glycoprotein F4/80

Fgf Fibroblast growth factor

Flk1 Fetal liver kinase 1

Foxa2 Forkhead box a2

Foxj1 Forkhead box J1

G

Gapdh Glyceraldehyde-3-phosphate dehydrogenase

Gm-csf granulocyte/macrophage stimulating factor

GPCR G protein coupled receptor

H

H&E hematoxylin and eosin

H₂O Water

HEPES 4-(2-hydroxyethyl)-1-piperazineethanesulfonic acid

Hif-1 α Hypoxia inducible factor 1 alpha subunit

Hopx HOP homeobox

I

Il Interleukin

L

LPS Lipopolysaccharide

LysM Lysozyme-M

M

Mac2 Galactose-binding lectin

miR MicroRNA

N

NaCl Sodium Chloride

NF- κ B Nuclear factor kappa B

Nkx2.1 Transcription factor NK2 homeobox 1

Nmyc bHLH transcription factor

O

ON Overnight

P

P	Postnatal day
PBS	Phosphate buffer solution
PCR	Polymerase chain reaction
Pdpr	Podoplanin
PFA	Paraformaldehyde
proSp-C	Precursor of surfactant protein C

Q

qPCR	Quantitative PCR
------	------------------

R

RNA	Ribonucleic acid
RT	Room temperature

S

Scgb1a1	Secretoglobin, family 1A, member 1
SDS	Sodium Dodecyl Sulfate
SEM	Standard error mean
Shh	Sonic hedgehog
Sox	Sex determining region Y -related HMG-box
Sp	Surfactant protein

T

TEBs	Terminal end buds
Tgf β	Transforming growth factor β
Tie2	Endothelial-specific receptor tyrosine kinase

V

VD	Volume density
Ve-cad	Vascular endothelial cadherin
Vegfa	Vascular endothelial growth factor

W

Wk	Weeks
Wnt	Wingless-type MMTV integration site family

Figure List

Figure 1- Adult human lung anatomy and cellular composition.....	4
Figure 2- Schematic representation of different lung stages.	5
Figure 3- Tissue macrophages origins in several organs.....	9
Figure 4- Schematic representation of lung slices cutting to test culture of two different fetal lung regions: all lung and distal lung.....	23
Figure 5- Distal epithelium transcripts expression analysis at canalicular stage (E16.5).	29
Figure 6- Distal epithelium transcripts expression analysis at saccular stage (E18.5).	30
Figure 7- Distal epithelium transcripts expression analysis at saccular stage (P0).	31
Figure 8- Aqp5 and proSp-C expression in <i>Csf1r</i> ^{-/-} lungs at saccular stage (E18.5).	33
Figure 9- Aqp5 and proSp-C expression in <i>Csf1r</i> ^{-/-} lungs at saccular stage (P0).	34
Figure 10- Proximal epithelium transcripts expression analysis at canalicular stage (E16.5).....	36
Figure 11- Proximal epithelium transcripts expression analysis at early saccular stage (E18.5).	37
Figure 12- Proximal epithelium transcripts expression analysis at saccular stage (P0).	38
Figure 13- Vascular mediators' transcripts expression analysis at canalicular stage (E16.5).....	39
Figure 14- Vascular mediators' transcripts expression analysis at early saccular stage (E18.5).	41
Figure 15- Vascular mediators' transcripts expression analysis at saccular stage (P0).	42
Figure 16- Ve-cad and Cd31 expression in <i>Csf1r</i> ^{-/-} lungs at early saccular stage (E18.5).	43
Figure 17- Ve-cad and Cd31 expression in <i>Csf1r</i> ^{-/-} lungs at early saccular stage (P0).	44
Figure 18- Different lung region slices and ascorbic acid supplementation affect tissue viability in culture.....	46
Figure S1- Drastic reduction of tissue macrophages in <i>Csf1r</i> ^{-/-} lungs.	71
Figure S2- Tissue macrophages disrupt lung morphology at fetal and post-natal saccular stage.	71

1. INTRODUCTION

1.Introduction

Lung development is a complex process that involves cellular, genetic and epigenetic mechanisms to achieve the maturity necessary to perform its mainly function: breath. Lung immaturity is a consequence of a preterm birth, and is the major cause of respiratory morbidity in child and adulthood¹. Moreover, bronchopulmonary dysplasia, a chronic lung disease consequence of respiratory distress in most of preterm births and is one of the major causes of preterm birth mortality²⁻⁴. Nowadays, glucocorticoids administration is performed in preterm infants to accelerate lung maturation⁵. However, glucocorticoids therapy has been associated with several adverse effects in child and adulthood, as impairments in pulmonary, nervous and cardiovascular systems^{5,6}. To better understand and develop new therapeutic approaches for these situations and others, firstly it is necessary to unravel more about cellular and molecular mechanisms of lung development.

1.1 Lung development

Respiratory system is constituted of nose, pharynx, trachea and lung. In lung, particularly in the alveoli, occur gas-exchange between alveoli and capillaries. Before air flow contact with alveoli, it passes by primary bronchi composed by basal cells, mucous/secretory cells, ciliated cells, neuroendocrine cells and dendritic cells (Figure 1). The following is the intralobar bronchi constituted by clara cells, ciliated cells, neuroendocrine cells, smooth muscle cells, goblet cells and dendritic cells (Figure 1). The last and peripheral region is the bronchioalveolar duct junction that opens to the alveoli (Figure 1). It is constituted by ciliated cells and clara cells in proximal region, and alveolar differentiated cells, fibroblasts, endothelial cells, pericytes and macrophages in distal region⁷. Ciliated cells and clara cells are responsible for host defense through microorganisms and extrinsic particles capture in mucous and consequent elimination by phagocytic cells (e.g. macrophages). Clara cells are also responsible for surfactant proteins synthesis and secretoglobulins production, important components of airway fluid⁸. Basal cells present a structural role in conducting airway structures and are responsible for the interaction with immune cells present in lung parenchyma⁷. Goblet cells are the source of mucous important to homeostasis maintenance and host defense⁷. Neuroendocrine cells are responsible for neurotransmitters production such as serotonin and calcitonin (Calca)⁷. The main function of this cells is to modulate lung growth and differentiation in fetal periods and are involved in cellular sensing (e.g. nicotine and hypoxia stimuli)⁹. Besides, neuroendocrine cells are found in clusters

called neuroepithelial bodies¹⁰. Fibroblasts are responsible for extracellular matrix components synthesis, and smooth muscle cells and pericytes are responsible for mechanistic lung movements¹¹⁻¹³. Macrophages are phagocytic immune cells present in lung since embryonic and fetal lung development stages and are responsible for host defense, alveoli clearance and production of pro-inflammatory cytokines¹⁴. Therefore, lung is a complex organ with a variety of cellular types, which anticipates highly elaborate regulatory mechanisms to its development.

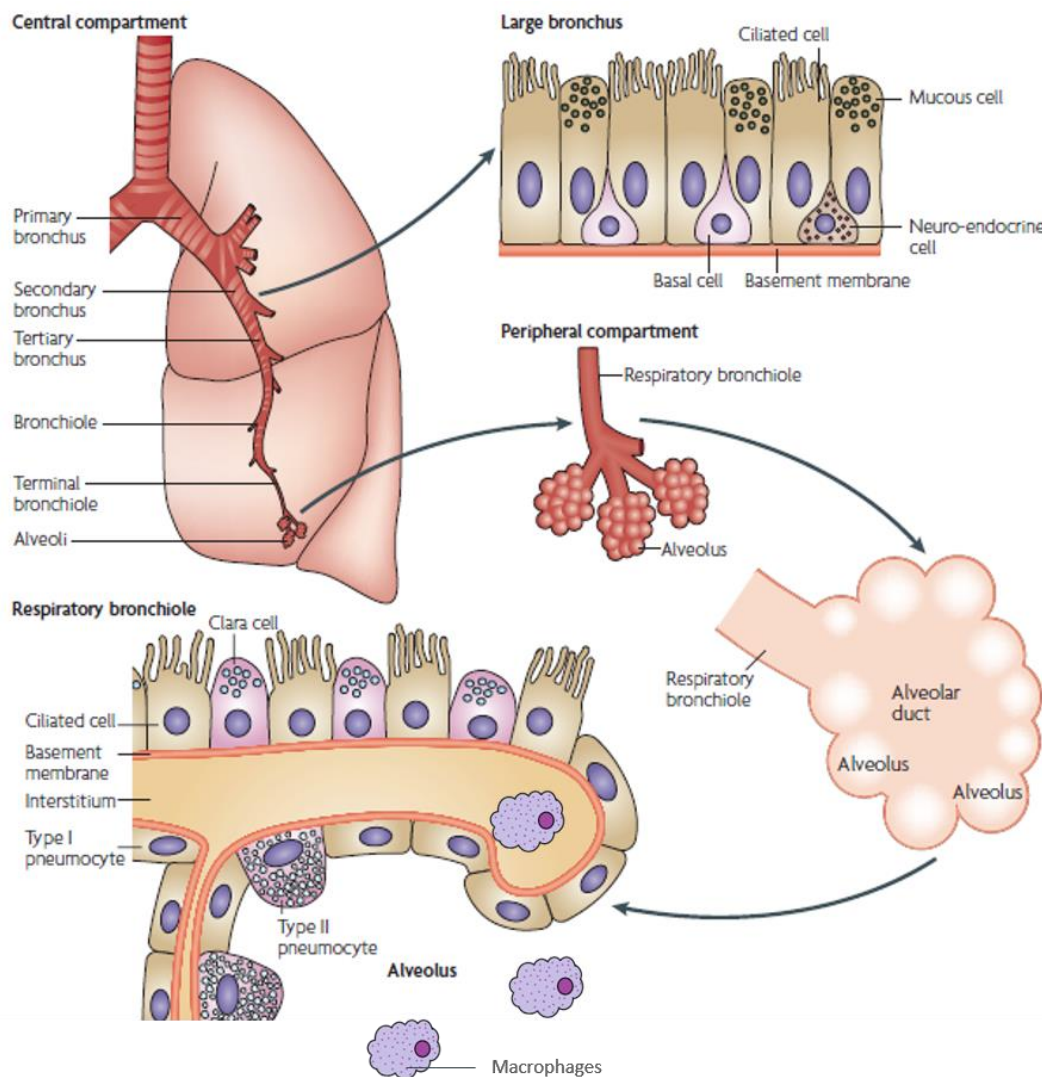


Figure 1- Adult human lung anatomy and cellular composition.

Lung is a complex organ constituted for a variety of cellular types necessary to a correct lung function. Adult lung is mainly composed by three specialized structures: bronchus, bronchioles and alveolus. Bronchi structure is composed by basal, ciliated, mucous and neuroendocrine cells. Bronchiole structure is composed by most cells present in bronchi and in addition with alveolar cells (also known as pneumocytes). Alveoli are mostly composed by alveolar cells, capillaries and macrophages. Image adapted from Sun et al. 2007⁸⁸.

Lung formation in mammals is studied mostly using rodent models, such as rat and mouse¹⁵. Although some anatomical differences exist between human and rodents, the known molecular processes in lung development events, as branching morphogenesis and differentiation, are been demonstrated to be similar between these species¹². Three right lobes and two left lobes compose human lung, while mouse lung is constituted by one left lobe and four right lobes. Another anatomical difference is the presence or absence of respiratory bronchioles in humans and rodents, respectively¹².

Lung development begins early in embryonic period and finishes only postnatally and is subdivided in five stages: embryonic (embryonic day (E) 9-11.5 in mice; 3-7 weeks (wk) in human), pseudoglandular (E11.5-16.5; 5-17 wk), canalicular (E16.5-17.5; 16-26 wk), saccular (E17.5-postnatal day (P) 5; 24-38 wk) and alveolar (P5-28; 38 wk – maturity)¹⁶ (Figure 2).

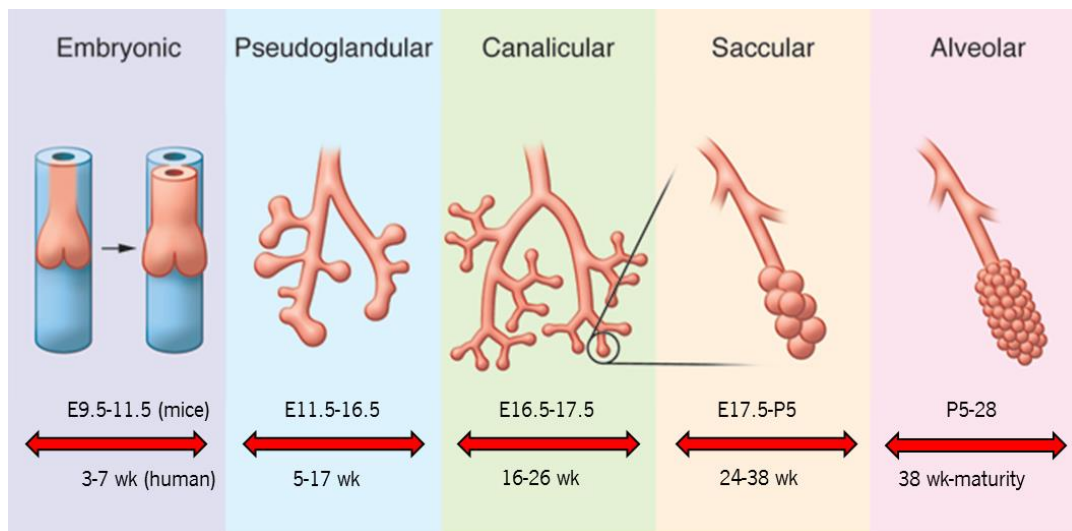


Figure 2- Schematic representation of different lung stages.

Embryonic stage is characterized by lung specification, followed by branching morphogenesis during pseudoglandular stage. Canalicular stage is characterized by respiratory bronchioles and alveolar ducts formation. In saccular stage occurs alveolar sacs formation and consequent sub-division to origin primitive alveolus, followed by alveoli primary septation and maturation. Alveolar stage is characterized by secondary septation and alveoli full maturation. Image adapted from Rackley et al. 2012¹⁵.

1.1.1 Airways unit development

The first known molecular regulatory event in respiratory system development is the transcription factor NK2 homeobox 1 (Nkx2.1) localized expression in the anterior foregut at E9¹⁷. Nkx2.1 expression is a morphogenic process highly regulated by Wingless-type MMTV integration site family (Wnt), bone morphogenetic protein (Bmp) and fibroblast growth factor (Fgf) signaling in lung

endoderm^{17,18}. At embryonic stage occurs two primitive lung buds formation (main bronchi formation) and division of trachea and esophagus development¹⁶. Surrounded mesenchyme originates the cartilage present in trachea and conducting airways¹⁶.

Vascular complex starts to develop at E9 from lung mesoderm. Two different processes occur during vasculature development in the lung: vasculogenesis and angiogenesis. Vasculogenesis is the process of blood vessel formation from endothelial progenitor cells, and angiogenesis is the formation of new blood vessels through the branching of preexisting vessels¹⁹. In the last two decades, pulmonary vasculature formation has been studied and there are different models that try to explain its formation. In 1997, deMello *et al.* described for the first-time vasculature development in lung. In this model, the peripheral blood vessels are formed by vasculogenesis, also called distal or peripheral vasculogenesis, from hematopoietic lakes present in the mesenchyme¹⁹. In this model, angiogenesis (also called central angiogenesis) occurs in the central region and it is the origin of arteries and veins¹⁹. Hall *et al.* suggested that capillary plexus is formed by distal vasculogenesis through angioblasts differentiation present in lung mesenchyme and not from hematopoietic lakes²⁰. In 2005, Parera *et al.* proposed a new concept and model to explain lung vasculature formation: distal angiogenesis. Pulmonary vasculature origin is based on sprouting of preexisting vessels in lung periphery, and consequently lung vasculature was formed by angiogenesis without occurring vasculogenesis²¹. More recently, it was described the existence of a cardiopulmonary mesoderm progenitors (CPP), a multipotent cell responsible for vascular and airways smooth muscle cells and proximal endothelium formation and it is regulated by sonic hedgehog (Shh) pathway²². Vascular plexus origin is from pulmonary arteries originated in heart outflow tract²². Moreover, CPPs are responsible for most of mesodermal cell lineages in lung²². Distal vasculature arises from vascular endothelial cadherin (Ve-cad) positive cells and not from CPP, demonstrating a different origin of proximal and distal lung vasculature formation²². Therefore, pulmonary vasculature formation is a complex process and probably occurs through a mix between vasculogenesis and angiogenesis processes.

Pseudoglandular stage is mainly characterized by proliferation and sub-division of main bronchi into a tree-like structure of terminal tubules, namely branching morphogenesis^{16,17}. Lung buds development is a repetitive cycle of four highly regulated processes: buds elongation, outgrowth cessation, tip expansion and bifurcation¹⁷. Branching morphogenesis occurs through different bifurcation orientation (domain, planar and orthogonal) to create that lung tree-like structure²³.

Mesodermal expression of Fgf10 is the major responsible for branching morphogenesis regulation. Its expression is highly regulated by Bmp-4, Shh, retinoic acid, Notch and transforming growth factor β (Tgf β), which reveals branching morphogenesis as a highly regulated complex process^{12,24}. Moreover, lung endoderm gives rise to two distinct epithelium cell lineages. Proximal epithelium progenitor cells express Sox2, a sex determining region Y -related HMG-box (Sox) family of transcription factors, that give origin to bronchiole differentiated cells: neuroendocrine cells, clara cells, ciliated cells and goblet cells¹⁸. Distal epithelium progenitor cells express Sox9 and give rise to alveolar cells type I and II (AT1 and AT2, respectively)¹⁸. In the end of pseudoglandular stage and early canalicular stage, the main cellular events are bronchiole differentiation^{12,15}.

The capillary plexus development proceed in concomitance with the airways epithelial branching development^{20,22}. At E14.5 and E16.5, vascular endothelial growth factor (Vegfa) is expressed in lung epithelial cells²⁵. Moreover, Fgf9 and Shh signaling pathways are responsible for Vegfa expression in lung mesenchyme, and consequently promoting vascular development²⁶. Impairments in vasculature formation lead to reduced branching morphogenesis in lung, suggesting a relationship between epithelium and vasculature formation during pseudoglandular stage²⁷.

In the end of pseudoglandular stage, the mainly events for airways unit formation are almost complete with the exception of secretory cells differentiation, that only begins during canalicular stage.

1.1.2 Respiratory unit development

Lungs respiratory unit is primarily composed by respiratory bronchioles and alveolar sacs. The formation of these structures begins in canalicular stage and mainly occurs at saccular and alveolar stages. Alveolar cells differentiation begins at canalicular stage, with enlargement of terminal bronchioles accomplished by respiratory bronchioles and alveolar ducts formation, including conducting airway cells differentiation (e.g. secretory cells)^{2,15}. Vasculature continue developing concomitantly with airways expansion through angiogenesis^{2,12}. Vegfa expression becomes restricted to distal epithelium and promotes vasculature expansion concomitantly with epithelial development²⁸. AT2 cells differentiation leads to the beginning of surfactant production¹².

At saccular stage occurs an enlargement of airspace areas concomitantly with alveolar sacs formation and consequent sub-division to origin primitive alveolus. Another main event is the distal epithelium differentiation (AT1 and AT2 cells differentiation) that has already started in the previous

phase¹⁶. AT2 differentiated cells produce surfactant proteins (Sp) namely Sp-A, Sp-B, Sp-C and Sp-D. These proteins have different functions in lung, including homeostasis maintenance, immunological response, and are crucially to prevent alveolar collapse^{29,30}. AT1 differentiated cells are responsible for gas-exchange in alveoli and are 95-97% of total peripheral lung area. Alveolar fluid composition and quantity is also modulated by AT1 cells³¹. Little is known about the regulatory mechanisms of alveolar differentiation. Recent studies are disclosing some molecular players in this cellular process during saccular and alveolar stage. AT1 and AT2 cells arise from a common bipotent progenitor cell, characterized by Sp-C and podoplanin (Pdpn) expression^{32,33}. Histone deacetylase 3 is a key player in AT1 cells spreading and remodeling through inhibition of miR-17-92. miR-17-92 is responsible for Tgf β signaling inhibition, which consequently promotes impairments in distal sacculation and alveolus remodeling³⁴. Type IV collagen is another molecule involved in alveolar differentiation and epithelial-endothelial interaction, due to regulate myofibroblasts differentiation, an essential cell population for a correct alveologenesis process³⁵. Notch signaling in epithelial cells is crucial during later saccular stage (P3) to alveolarization process³⁶. Inhibition of Notch signaling promoted enlarged airspaces, less secondary septation and decreased proliferative activity in AT2³⁶. Notch2 is highly expressed in AT2 cells at E18.5, and it is necessary to AT2 cells maturation in alveoli formation³⁶. Also, Wnt signaling is responsible for differentiation of a specific set of AT2 cells, the Axin2 positive cells, to mature AT2 cells and not to mature AT1 cells, suggesting Wnt signaling as a crucial regulator of alveolar differentiation during late saccular and alveolar stage³⁷. Moreover, keratinocyte growth factor (also known as Fgf7) promoted AT2 maturation through increasing Sp transcripts expression and surfactant phospholipids synthesis³⁸. Deletion of forkhead box a2 (Foxa2) promoted respiratory syndrome distress after 2-3 hours after birth³⁹. No morphological differences are seen in E15.5 or E18.5 *Foxa2*^{-/-} lungs, however alveolar differentiation is affected since E18.5 with decreased mature AT1 cells and an accumulation of AT2 immature-like cells³⁹.

Alveolar stage differs between human and mice because in humans alveolar stage begins before birth and in mice occurs at P5¹⁶. Alveolar stage is mainly characterized by alveolar and distal vasculature full maturation, and also mucous and basal cells differentiation^{15,16}. Not all the mechanisms of lung development are completely clear, and crosstalk between different cell populations are still unknown.

1.2 Tissue macrophages during organs development

In the last decades, there is a particularly interest in understanding the function of tissue macrophages during development, homeostasis and disease. Tissue macrophages are present in organs since E9 and accordingly to the organ that they populate, they present different transcriptional profiles⁴⁰⁻⁴². In general, tissue macrophages can be derived from yolk sac, fetal liver and bone marrow (Figure 3)⁴¹ and its differentiation signaling is performed mainly through activation of Csf1 receptor (Csf1r) via colony stimulating factor-1 (Csf1), or alternatively via interleukin-4 (IL-4)^{41,43,44}. Moreover, Csf1 signaling is responsible for proliferation, spreading, motility and survival of macrophages⁴⁴.

1.2.1. Tissue macrophages and organogenesis

The importance of tissue macrophages during embryonic development is already described to several organs. Most of these studies were associated with tissue macrophages differentiated by Csf1 signaling pathway.

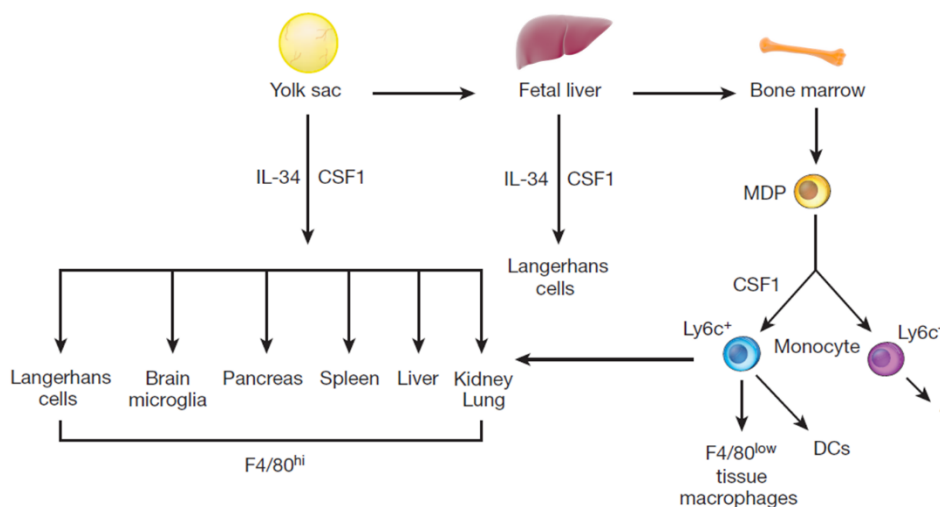


Figure 3- Tissue macrophages origins in several organs.

Tissue macrophages are a heterogeneous population present in several organs since embryonic stages presenting different origins. Bone marrow-derived macrophages are the classical lineage of macrophages activation throughout circulating blood monocytes differentiation occurring only after birth. Fetal liver and yolk sac are the major sources of tissue macrophages origin that populate and self-maintain in the different organs during adult life. Image adapted from Wynn, Chawla and Pollard, 2013⁴¹.

Using a transgenic model with enhanced green fluorescence protein (EGFP) associated to *Csf1r* promoter it was possible to follow tissue macrophages migration from yolk sac to organs in development, such as brain, kidney and lung⁴⁵. *Csf1r*-positive cells appear firstly at E9-9.5 in yolk sac, and at E11.5 are present in head's vasculature development⁴⁶. In kidney, *Csf1r*-positive cells co-localized with F4/80, a tissue macrophages marker⁴¹, closely to ureteric buds. Kidney explants with *Csf1* supplementation and low concentrations of lipopolysaccharide (LPS) presented increasing number of branch tips and nephrons, probably due to an increase in macrophages number in kidney explants⁴⁵.

In pancreas, tissue macrophages are present since E12.5 and pancreatic explants showed that *Csf1* stimulation promote an increase in macrophages number and in β endocrine cells, responsible for insulin production⁴⁷. Banaei-Bouchareb et al. also showed the influence of pancreatic tissue macrophages in β endocrine cells development through the use of a homozygous null mutation of *Csf1* (*Csf1*^{op/op}) mice⁴⁸. These mice showed decrease in insulin mass cells, probably due to decrease in insulin cell size and proliferative activity, and to increase in apoptosis⁴⁸.

Macrophages are present since the beginning of mammary gland development at the terminal end buds (TEBs)⁴⁹. Presence of apoptotic bodies in macrophages' cytoplasm of these areas suggests a clearance function of death epithelial cells⁴⁹. Using a homozygous null mutation in *Csf1* mice model, it was demonstrated that absence of tissue macrophages in mammary gland development promotes a decrease in TEBs formation, with decreased number of ducts and disorganized orientation⁴⁹. Administration of CSF1 human recombinant protein rescues normal mammary gland phenotype⁴⁹.

Hindbrain vasculature formation is also modulated by tissue macrophages. Absence of tissue macrophages promotes impairments in vascular anastomosis⁴⁶. Macrophages are chaperones between *Vegfa* endothelial tips fusion, a process called anastomosis, and essential to a correct vasculature formation⁴⁶. Moreover, *Csf1r* knockout gene (*Csf1r*^{-/-}) mice present impairments in normal hindbrain development, due to a completely absence of microglia (tissue macrophages of brain)⁵⁰. Moreover, brain architecture and periventricular zone formation are disrupted in *Csf1r*^{-/-} mice⁵⁰. In *Csf1*^{op/op} mice, hypothalamic-pituitary-gonadal axis is dysregulated and consequently induce impairments in luteinizing hormone production, a hormone responsible for testosterone synthesis in males and for estrogen positive feedback in females, a crucial process to ovulation⁵¹. Hypothalamus impairments are the cause of reproductive defects in these animal models⁵¹.

Bone development is also influenced by *Csf1r*-positive tissue macrophages, because *Csf1r*^{-/-} mice are osteoporotic⁵², with impaired bone remodeling as consequence of failure of osteoclasts, bone tissue macrophages, to resorb bone⁵². Macrophages ablation using a conditional knockout for Lysozyme-M (LysM), a protein expressed by myeloid cell lineage including monocytes and macrophages, promote smaller body size and, smaller and thinner bones⁵³. Moreover, macrophages are also important in bone injury recover⁵³.

All these evidences highlight these immunological cells as key players in the modulation of epithelial, endocrine and vasculature formation and differentiation.

1.2.2. Tissue macrophages and lung development

Adult lung presents two major types of tissue macrophages: alveolar macrophages and interstitial macrophages^{14,54}. Alveolar macrophages are present in alveolar airspaces and are involved in host defense, alveoli clearance and production of pro-inflammatory cytokines¹⁴. Interstitial macrophages are in the lung parenchyma adjacent to alveolar cells and with constantly interaction with dendritic cells and interstitial lymphocytes¹⁴.

During embryonic development, tissue macrophages migrate to lung in embryonic developmental stage (E9-10). There are two waves of fetal lung tissue macrophages: the first one arises in the beginning of lung development, is characterized by high levels of F4/80 expression and derived from yolk sac^{14,54}. The second wave appears around E14-15, is defined by low/intermediate levels of F4/80 expression and high levels of Mac2 expression, and arises from fetal liver. Mac2 is a galactose-binding lectin present in macrophages⁵⁵ and, F4/80 is a EGF-TM7 member of the adhesion-GPCR family and a classical macrophage marker⁵⁶. Adult alveolar macrophages differentiate from colony stimulating factor - 2 (Csf2) signaling activation in postnatal periods, and *Csf2* full knockout animals did not present any lung formation impairments during fetal period^{14,57,58}. However, fetal alveolar (Mac2-positive) and “primitive” interstitial macrophages (F4/80^{high}-positive) derived from yolk sac and fetal liver, respectively, are *Csf1r*-positive cells⁵⁴.

Tissue macrophages produce cytokines and chemokines responsible for organs modulation, such as interleukin (Il)-6 and Tgfβ⁴³. For example, in lung it is known that Il-6 modulates branching morphogenesis at early stages of lung development⁵⁹ and that Tgfβ is an alveolar remodeling and spreading modulator³⁴. Moreover, nuclear factor kappa B (NF-κB) signaling activation in fetal tissue macrophages disrupt airway morphogenesis⁶⁰. However, tissue macrophages function during

normal lung development remains unclear, as well as which processes could be modulated by these cells. As mentioned before, the main lung developmental events are branching morphogenesis and epithelium and vasculature differentiation and maturation. Taking in consideration the influence of tissue macrophages in other organs, our question is: are fetal lung tissue macrophages orchestrating lung formation and, which processes are they regulating across lung development?

In our laboratory, lungs of macrophage-deficient mice, *Csf1r*^{-/-}, presented deep tissue macrophages depletion in fetal lung, more than 85% decrease in F4/80 positive cells (Figure S1, supplementary information).

Histological analysis at E15.5, E18.5 and P0 evidences lung morphology disruption at E18.5 and P0 (unpublished data) on macrophage-deficient mice lungs. *Csf1r*^{-/-} mice showed reduced epithelial-like cells and airspace, increased non-epithelial-like cells and thickened septa (Figure S2, supplementary information). These findings comply us to conclude tissue macrophages are critical players in lung sacculation and distal epithelium events.

2.AIMS

2.Aims

Preterm birth is associated with high morbidity rates both in child and adulthood, mostly due to lung immaturity, which causes deficits in alveolar differentiation, a crucial process that occurs during saccular and alveolar stages of lung development. The available therapy to accelerate lung maturation has been demonstrated to cause adverse effects in some organs development. In this way, there is an urgent need to develop new therapeutic approaches to promote lung maturation. A better understanding of the complex cellular and molecular processes involved in lung development can bring important insights to this clinical context.

Tissue macrophages are key regulatory cells in several organs development, probably due to mediator's release accordingly to the microenvironment that are inserted. Our unpublished data showed clear distal epithelial and sacculation impairments in lungs *Csf1r*^{-/-} mice, which had a drastic reduction on tissue macrophages. These findings suggest that tissue macrophages are modulators of lung saccular stage development. In this way, it is fundamental to discover which lung developmental events are tissue macrophages influencing, namely in the saccular phase.

The main goal for this work was to unravel tissue macrophages function in epithelium differentiation and vasculature formation during lung development. Through using a tissue macrophage-deficient mice model (*Csf1r*^{-/-}), we intended to understand the cellular impairments consequent of tissue macrophages absence in lung during saccular stage. For the present master thesis work, we aimed specifically to:

1. Understand the effect of tissue macrophages absence in alveolar differentiation by evaluation of distal epithelium-related transcripts expression and of protein expression of AT1 and AT2 markers;
2. Unravel tissue macrophages function in proximal epithelium differentiation through assessment of proximal epithelium-related transcript expression;
3. Characterize tissue macrophages effect in vasculature formation with transcripts expression analyses of vascular mediators and protein expression quantification of endothelial cell markers.

3.MATERIALS AND METHODS

3. Materials and methods

3.1 Animals, Ethics and Tissue collection

All animal experiments were performed accordingly to the European Union Directive 2010/63/EU, and approved by the local ethics committee (023/2016). Animals were housed in standard cages (267 x 207 x 140mm) with 370 cm² floor area and five animals per cage (males and females separated) with controlled environment (55% of humidity, 22-24°C and 12h lights' cycle). The food and water were sterilized and available ad libitum. The colony was maintained in inbred and the microbiological state was conventional. In these experiences both animal genders were used. The mice strain used was *Csf1r* null (*Csf1r*^{-/-}), where *Csf1r* gene was inactivated⁸², in the background of C57BL/6J:C3Heb/FeJ (supplied by Prof. Richard Stanley, Albert Einstein College of Medicine, NY, USA). *Csf1r*^{-/-} males and females were crossed by the end of the day and separated in next morning, and we considered that day as E0.5. At E16.5, E18.5 and P0, pregnant females were sacrificed by cervical dislocation, embryos removed and decapitated. Lungs were dissected under a stereomicroscope and a piece of tissue was collected to perform DNA extraction and genotyping by polymerase chain reaction (PCR). Lungs for RNA extraction were immediately collected to liquid nitrogen and stored at -80°C. Lungs for immunofluorescence assays were processed during four days, first day in 4% paraformaldehyde (PFA) solution and in the followings in sucrose gradient solutions, and in the end frozen in gelatin-sucrose solution in liquid nitrogen, stored at -20°C and posteriorly sectioned in cryostat. All analyses were performed in 2 groups of animals, *Csf1r*^{+/+} and *Csf1r*^{-/-}, using a minimal of 5 independent litters containing both animals' groups.

3.2 DNA extraction and Genotyping PCR

A piece of tissue from fetuses and newborns were incubated in a lysis buffer solution (NaCl 0.2 M, SDS 0.2%, Tris 0.1 M pH 8.0, EDTA 5 mM) and proteinase K (0.09 mg/ml, Ref:3115879001, Roche) at 55 °C overnight (ON), followed by centrifugation at 13 000 rpm during 10 minutes. Supernatant was collected and isopropanol was added in the same volume proportion, followed by vortex and centrifugation at 13 000 rpm during 5 minutes. Supernatant was discarded and DNA pellet was dried during 1 hour at room temperature (RT) and was hydrated with H₂O nuclease-free. PCR for genotyping was performed using Supreme NZYtaq 2x Master Mix (Ref:MB05402, NZYTech); specific primers for *Csf1r* gene: AGACTCATTCCAGAACCAGAGC; GAATTTGGAGTCCTCACCTTTG; CCGGTAGAATTCCTCGAGTCTA; and 1 µL of DNA (≈50 ng/µL). PCR reaction included the following steps: a first step of 5 minutes at 92°C, 35 cycles of 20

seconds at 94°C, 45 seconds at 58°C and 1 minute at 72°C, and a last step of 7 minutes at 72°C. PCR products were analyzed by electrophoresis agarose gel and the following sizes were obtained and used to distinguish the 3 mice groups: *Csf1r*^{+/+}: 385 bp; *Csf1r*^{+/-}: 385 bp and 308 bp; *Csf1r*^{-/-}: 308 bp.

3.3 Reverse transcriptase -quantitative PCR

3.3.1 RNA extraction

Lungs at E16.5, E18.5 and P0 were immersed in TRIzol reagent (Ref:15596-026, Invitrogen) and tissue homogenate was obtained by mechanical disruption using microcentrifuge pestle and after needles with crescent gauge values. Homogenate was incubated at RT during 5 minutes, followed by chloroform addition (0.2 ml per 1 ml of TRIzol used before) and incubation at RT during 3 minutes. Samples were centrifuged (13 000 rpm during 15 minutes at 4 °C) and aqueous phase removed, and 100% isopropanol was added 1:1 proportion followed by incubation at RT during 10 minutes and centrifugation (13 000 rpm during 10 minutes at 4 °C). Supernatant was discarded and RNA pellet was washed with 70% ethanol, followed by centrifugation (8000 rpm during 5 minutes at 4 °C). Supernatant was discarded and RNA pellet let it dry during 15 minutes and was hydrated with H₂O RNase-free.

3.3.2 cDNA conversion

To convert 2 µg of RNA it was used the commercial Maxima First Strand cDNA synthesis kit (Ref:K1671, Thermo Fisher Scientific), following the manufacturer instructions. Briefly, genomic DNA residues were eliminated using a reaction solution containing 10x DNase Buffer, dsDNase and RNA template at 37 °C during 2 minutes. cDNA conversion was performed using a reaction solution containing 5x reaction mix and Maxima Enzyme, Reverse Transcriptase, followed by 10 minutes at 25 °C, 20 minutes at 50 °C and 5 minutes at 85 °C.

3.3.3 qPCR

cDNA was mixed with commercial 2x Maxima Probe/ROX Master Mix (Ref: K0231, Thermo Fisher Scientific), containing a Hot Start Taq DNA Polymerase, and TaqMan® Gene Expression assay, specifically *Gapdh* (Ref:Mm99999915_g1, Thermo Fisher Scientific), *Sox9* (Ref:Mm00448840_m1, Thermo Fisher Scientific), *E-cad* (Ref:Mm01247357_m1, Thermo Fisher Scientific), *Pdpr* (Ref: Mm01348912_g1, Thermo Fisher Scientific), *Aqp5* (Ref:Mm00437578_m1, Thermo Fisher Scientific), *Hopx* (Ref:Mm00558630_m1, Thermo Fisher Scientific), *Abca3* (Ref:Mm00550501_m1, Thermo Fisher Scientific), *Sp-B*

(Ref:Mm00455678_m1, Thermo Fisher Scientific), *Sp-C* (Ref:Mm00488144_m1, Thermo Fisher Scientific), *Sp-D* (Ref:Mm00486060_m1, Thermo Fisher Scientific), *Sox2* (Ref:Mm03053810_s1, Thermo Fisher Scientific), *Scgb1a1* (Ref:Mm00442046_m1, Thermo Fisher Scientific), *Foxj1* (Ref:Mm01267279_m1, Thermo Fisher Scientific), *Calca* (Ref:Mm00801463_g1, Thermo Fisher Scientific), *Fgf2* (Ref:Mm00433287_m1, Thermo Fisher Scientific), *Hif-1 α* (Ref:Mm01283760_m1, Thermo Fisher Scientific), *Ang1* (Ref:Mm00456503_m1, Thermo Fisher Scientific), *Ang2* (Ref:Mm00545822_m1, Thermo Fisher Scientific), *Ve-cad* (Ref:Mm00486938_m1, Thermo Fisher Scientific), *Flk1* (Ref:Mm01222421_m1, Thermo Fisher Scientific), *Vegfa* (Ref:Mm01281449_m1, Thermo Fisher Scientific) and *Cd31* (Ref:Mm01242584_m1, Thermo Fisher Scientific). Quantitative PCR (qPCR) thermocycler program was 10 minutes at 95°C, 40 cycles of 15 seconds at 95 °C and 30 seconds at 60 °C. Transcript levels were normalized to endogenous control *Gapdh* and transcripts expression levels analysis was performed accordingly to $2^{-\Delta\Delta CT}$ method⁶¹. Gene expression data was presented in % relative transcript expression based on: $2^{-\Delta\Delta CT}$ (individual value) / average ($2^{-\Delta\Delta CT}$ (*Csf1r*^{+/+} group)) * 100. Statistical analysis was performed using % relative transcript expression (*Csf1r*^{+/+} group) vs % relative transcript expression (*Csf1r*^{-/-} group). E16.5: N (*Csf1r*^{+/+}) = 13; N (*Csf1r*^{-/-}) = 9; E18.5: N (*Csf1r*^{+/+}) = 12; N (*Csf1r*^{-/-}) = 12; P0: N (*Csf1r*^{+/+}) = 10; N (*Csf1r*^{-/-}) = 8.

3.4 Immunofluorescence

3.4.1 Immunofluorescence of alveolar epithelial cells markers

To analyze alveolar differentiation during saccular stage (E18.5 and P0), protein expression of aquaporin-5 (Aqp5) and precursor Sp-C (proSp-C) were assessed by immunofluorescence. Lung frozen section slides (around 20 μ m) were defreeze during 30 minutes and were fixated with 4% PFA during 20 minutes. Permeabilization was performed with 0.3 % Triton X-100 (Ref:93420, Thermo Fisher Scientific) and 1% bovine serum albumin (BSA) (Ref:A7906, Sigma-Aldrich) in phosphate buffer solution (PBS) 1x solution during 1 hour. Antigen retrieval was performed using citrate buffer 10 mM pH=6 during 15 minutes (5+5+5) in microwave at 600 W. Unspecific antigen binding blocking was performed with normal horse serum (1/10, Ref:H0146, Sigma-Aldrich) and normal donkey serum (1/5, Ref:D9663, Sigma-Aldrich) in PBS 1x during 1 hour. ProSp-C rabbit anti-human primary antibody (1/1000, Ref:ab3786, Sigma-Aldrich) was incubated ON at RT, followed by biotinylated horse anti-rabbit secondary antibody during 2 hours (1/250, Ref:BA-1100, Vector Labs) and Streptavidin-Alexa Fluor® 568 conjugate during 1 hour (1/200, Ref:S11226,

Invitrogen). Next, Aqp5 rabbit anti-mouse primary antibody (1/250, Ref:ab78486, Invitrogen) was incubated ON at RT, followed by DyLight™ 488 Donkey anti-rabbit secondary antibody (1/250, Ref:YC2.406404, Biolegend) incubation during 2 hours. Nuclear staining was performed next using 4',6-Diamidino-2'-phenylindole dihydrochloride (DAPI) (1/1000, Ref:D1306, Invitrogen) by 5 minutes incubation at RT. Slides were mounted with PermaFluor™ Aqueous Mounting Medium (Ref:TA-006-FM, Invitrogen). E18.5: N (*Csf1r*^{+/+}) = 12; N (*Csf1r*^{-/-}) = 9; P0: N (*Csf1r*^{+/+}) = 10; N (*Csf1r*^{-/-}) = 8.

3.4.2 Immunofluorescence of endothelial cells markers

To analyze vasculature formation during saccular stage, protein expression of platelet endothelial cell adhesion molecule (Cd31) and Ve-cad was assessed by immunofluorescence. Lung frozen section slides defreeze during 30 minutes, followed by antigen retrieval was performed using citrate buffer 10 mM pH=6 during 15 minutes (5+5+5) in microwave at 600 W. Unspecific antigen binding blocking was performed with normal horse serum (1/10, Ref:H0146, Sigma-Aldrich) and normal donkey serum (1/5, Ref:D9663, Sigma-Aldrich) in PBS1x during 1 hour. Cd31 goat anti-mouse (1/250, Ref:sc-1506, SantaCruz) were incubated ON at RT, followed for biotinylated horse anti-goat during 2 hours (1/500, Ref:BA-9500, Vector Labs) and Streptavidin-Alexa Fluor® 568 conjugate during 1 hour (1/200, Ref:S11226, Invitrogen). Next, Ve-cad goat anti-mouse (1/250, Ref:ab78486, Invitrogen) was incubated ON at RT, followed by Alexa Fluor® 488 Donkey Anti-Goat (1/500, Ref:A11055, Invitrogen) incubation during 2 hours. Nuclear staining was performed using DAPI (1/1000, Ref:D1306, Invitrogen) during 5 minutes at RT. Lung slides were mounted with PermaFluor™ Aqueous Mounting Medium (Ref:TA-006-FM, Invitrogen). E18.5: N (*Csf1r*^{+/+}) = 12; N (*Csf1r*^{-/-}) = 9; P0: N (*Csf1r*^{+/+}) = 10; N (*Csf1r*^{-/-}) = 8.

3.4.3 Confocal microscopy and quantitative analysis

To quantify protein expression area of Aqp5, proSp-C, Cd31 and Ve-cad, representative images from lung tissue sections (20% of total lung tissue) were taken using Olympus FluoView™ FV1000 confocal microscope at 60x oil objective. Protein positive areas and all lung parenchyma area (DAPI positive) were quantified using ImageJ 1.50i software. Using threshold function available on ImageJ, it was possible to measure the different areas in the different filters (red, green and blue) in a grey scale image (RGB stack option). Area quantification values were measured in an arbitrary unit. Positive expression area was presented as positive protein area/ DAPI positive area.

3.5 Tissue culture

3.5.1 Lung slices culture

Wild-type males and females (C57BL/6J:C3Heb/FeJ background) were crossed by the end of the day and separated in next morning, and it was considered that morning as E0.5. At E16.5, pregnant females were sacrificed by cervical dislocation, embryos removed and decapitated. Lungs were dissected under a stereomicroscope inside of a sterile vertical flow chamber. Left lung slices were obtained using a n°11 blade (0.5-1mm³) and a slim scissor, and cultured in Dulbecco's Modified Eagle Medium: Nutrient Mixture F-12 (DMEM/F12) (Ref:733-1668, Lonza), penicillin/streptomycin (1%, Ref:P4333, Sigma-Aldrich), 4-(2-Hydroxyethyl)piperazine-1-ethanesulfonic acid, N-(2-Hydroxyethyl)piperazine-N'-(2-ethanesulfonic acid) (HEPES) (15 mM, Ref:H4034, Sigma-Aldrich) over a isopore membrane filter 0.4 μm (Ref:HTTP01300, Merck), previously hydrated with DMEM/F12 (733-1668, Lonza) for at least 1 hour. Different conditions were tested: ascorbic acid supplementation (0.2 mg/ml, Ref:A92902, Sigma-Aldrich); and slices derived from different lung regions, all left lobe lung and distal lung, as schematized in figure 4. Lung slices were cultured during 24 and 48 hours at 37 °C with 5 % of CO₂. N (all left lobe with ascorbic acid) = 4; N (all left lobe without ascorbic acid) = 4; N (distal lung with ascorbic acid) = 3 and N (distal lung without ascorbic acid) = 5.

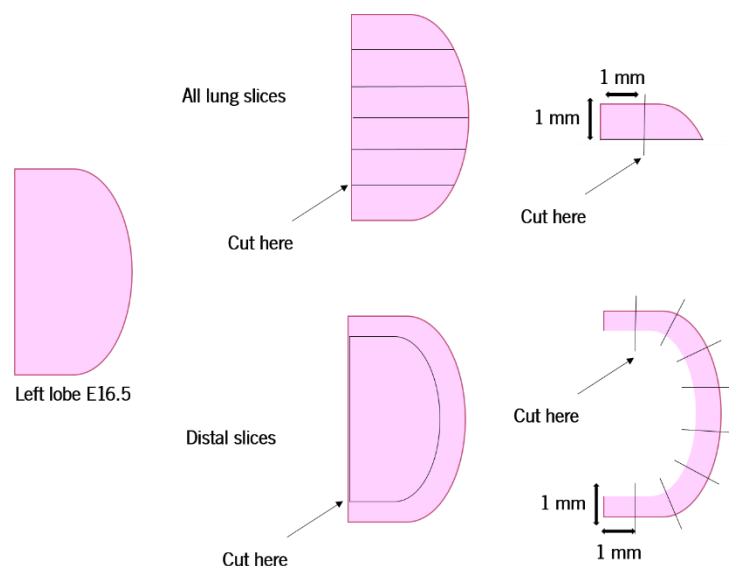


Figure 4- Schematic representation of lung slices cutting to test culture of two different fetal lung regions: all lung and distal lung

3.5.2 Tissue processing, microscopy and cell death analysis

After 24 or 48 hours of culture, lung slices were collected in 4 % PFA, incubated ON at RT, and processed to formalin-fixed paraffin-embedded tissue. Next, lungs slices were sectioned (3 μ m) and submitted to hematoxylin and eosin (H&E) staining. To quantify apoptotic bodies in lung slices stained with H&E, representative images from lung tissue sections (20% of total tissue) were taken using an Olympus DP70 photographic camera linked to Olympus BX 81 microscope at 20x and 40x objectives. Apoptotic bodies were identified accordingly to specific histologic characteristics (small vesicles with dark purple coloration)⁶². Apoptotic bodies areas and lung parenchyma areas were quantified using selection function of ImageJ 1.50i software. Area quantification values were measured in an arbitrary unit. Apoptotic bodies area was normalized to lung parenchyma area: apoptotic bodies area / lung tissue area.

3.6 Statistical analysis

All data was presented as mean \pm standard error mean (SEM). Simple comparisons between *Cs1r*^{+/+} and *Cs1r*^{-/-}; and simple comparisons between different lung culture conditions were performed using Two-tailed Student's t-test: *p < 0.05, **p < 0.01 and ***p < 0.0001 in GraphPad Prism version 5.0.

4.RESULTS

4.RESULTS

Tissue macrophages are involved in the modulation of several organ developmental processes (kidney⁴⁵, bone⁵³, brain⁴⁶, pancreas⁴⁷, and mammary gland⁴⁹), particularly in branching morphogenesis and vasculature formation. In lung, fetal tissue macrophages activation through NF- κ B signaling disrupted fetal airways morphogenesis⁶⁰. However, it is unknown the contribution of fetal tissue macrophages to normal lung development. In this work, we used a knockout animal for *Csf1r* gene, that is a membrane receptor responsible for tissue macrophage differentiation throughout Csf1 signaling^{41,43,44}, in order to understand which are the mainly cellular alterations modulated by tissue macrophages across lung development.

Unpublished data from the group show that *Csf1r*^{-/-} fetal lungs at saccular stage (E18.5 and P0) exhibit decreased alveolar airspaces area and increase of non-epithelial-like cells, being this phenotype even more pronounced after birth (P0) (Figure S2, supplementary information). Moreover, these analyses show the existence of different levels of lung phenotype severity, with the majority of *Csf1r*^{-/-} fetal lungs with a high severity degree of the mentioned impairments and some with a mild to moderate degree. The lung tissue macrophage deficiency of this model was confirmed by immunofluorescence using a classical macrophage marker, F4/80⁵⁴. The deficiency in the fetal saccular lungs was confirmed by a reduction of more than 85% in F4/80+ tissue macrophages in *Csf1r*^{-/-} lungs (unpublished data) (Figure S1, supplementary information). However, it is unknown which cellular and molecular processes are modulated by fetal tissue macrophages in lung formation.

4.1 Tissue macrophages involvement in alveolar differentiation

Tissue macrophages were involved in the modulation of epithelial pancreatic tissue, specifically β -cells proliferation and differentiation⁴⁷. Lung development occur through bronchial-tree branching, as occur in kidney and mammary gland, and its function is dependent on the correct development of the epithelium (bronchial and alveolar cells differentiation). So, we hypothesized that tissue macrophages are involved in alveolar epithelial differentiation. To confirm this, we decided to investigate alveolar differentiation throughout canalicular (E16.5) and saccular stage (E18.5 and P0) in lung tissue of *Csf1r*^{-/-} mice.

Initially, we assess transcript expression levels of cell type-specific markers: progenitor distal cells (*Sox9*), epithelial cells (*E-cad*), AT1 (*Pdpr*, *Aqp5* and *Hopx*) and AT2 (*Abca3*, *Sp-B*, *Sp-C* and *Sp-D*) cells by RT-qPCR. Since, alveolar differentiation is a process that initiates in the canalicular stage, and mainly occurs during saccular stage¹⁷, we will perform this analysis at E16.5 (begin of canalicular stage), E18.5 (early

saccular stage) and P0 (saccular stage). All the transcripts relative expression levels of *Csf1r*^{-/-} mice were compared to *Csf1r*^{+/+} mice at the same timepoint.

At E16.5, *Sox9* expression was not affected in *Csf1r*^{-/-} animals (101.2±3.48 vs 100.0±2.16, *p*=0.7503) (Figure 5). The epithelial compartment showed a statistical increase in *E-cad* transcript expression (14%; 113.9±4.741 vs 100.0±1.38, *p*=0.0029) (Figure 5). *Pdpr* is a mucin-type transmembrane protein expressed in alveolar bipotential progenitor cells and AT1 mature cells³³, and its transcript expression was statistically slight increase in *Csf1r*^{-/-} mice (7%; 106.5±2.19 vs 100.0±1.48, *p*= 0.0195) (Figure 5). *Aqp5* is a member of aquaporin family and it is expressed in apical plasma membrane of AT1 cells³¹. *Aqp5* transcript levels were not altered (102.8±5.04 vs 100.0±5.642, *p*=0.7279) (Figure 5). *Hopx* is a member of homeodomain-containing protein family⁶³, and it is expressed in AT1 cells since E15.5⁶⁴. *Hopx* was statistically increased (22%; 121.7±8.547 vs 100.0±2.68, *p*=0.0088) (Figure 5). Most of AT2 transcripts presented higher transcript expression levels in *Csf1r*^{-/-} lungs (*Abca3* (25%): 124.8±8.01 vs 100.0±1.29, *p*=0.0023; *Sp-B* (44%): 143.7±17.14 vs 100.0±2.33, *p*=0.0062; *Sp-C* (28%): 127.9 ± 10.68 vs 100.0±4.63, *p*=0.0146), except *Sp-D* transcript, which did not present statistical differences (105.1±12.21 vs 100.0±4.11, *p*=0.6485) (Figure 5). Interestingly, *Sp-D* transcript levels presented two distinct expression patterns in *Csf1r*^{-/-} group that divided it in two. A sub-group, designated as *Csf1r*^{-/-} up, showed a significant augment in *Sp-D* transcript levels (34%; 134.1±10.86 (N=4) vs 100.0±4.11(N=12), *p*=0.0026), and another subgroup, denominated *Csf1r*^{-/-} down, a decreased expression of this transcript expression levels (24%; 76.21±4.50 (N=4) vs 100.0±4.11 (N=12), *p*=0.0078). As already mentioned, different lung morphological severities were observed in *Csf1r*^{-/-} lung phenotypes, so it was not a surprise that different expression patterns could occur. At E18.5, a first analysis showed that *Csf1r*^{-/-} transcript expression patterns were very heterogeneous (Figure 6A) with 2 sub-groups for almost all the genes (Figure 6B), as observed in *Sp-D* transcript expression levels at E16.5. Only *Sp-C* transcript levels presented a statistically increase in all *Csf1r*^{-/-} group (31%; 131.3±9.78 vs 100.0±2.43, *p*=0.0061) (Figure 6A). A detailed analysis of *Csf1r*^{-/-} sub-groups was performed in the remaining genes. In *Csf1r*^{-/-} up sub-group, *Sox9* was 74% (173.7±17.32 (N=4) vs 100.0±4.23 (N=10), *p*<0.0001) and *E-cad* 54% increased (153.9±20.30 (N=6) vs 100.0±5.20 (N=10), *p*=0.0046) (Figure 6B).

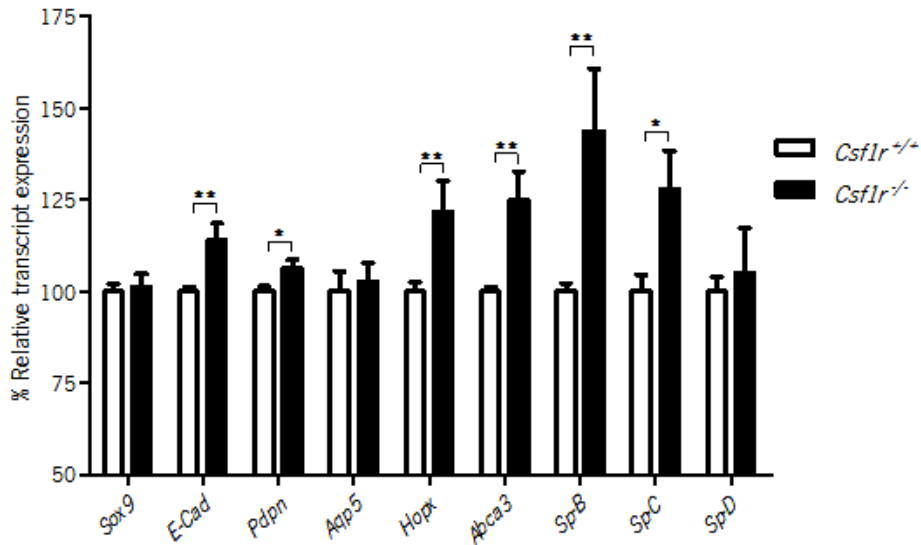
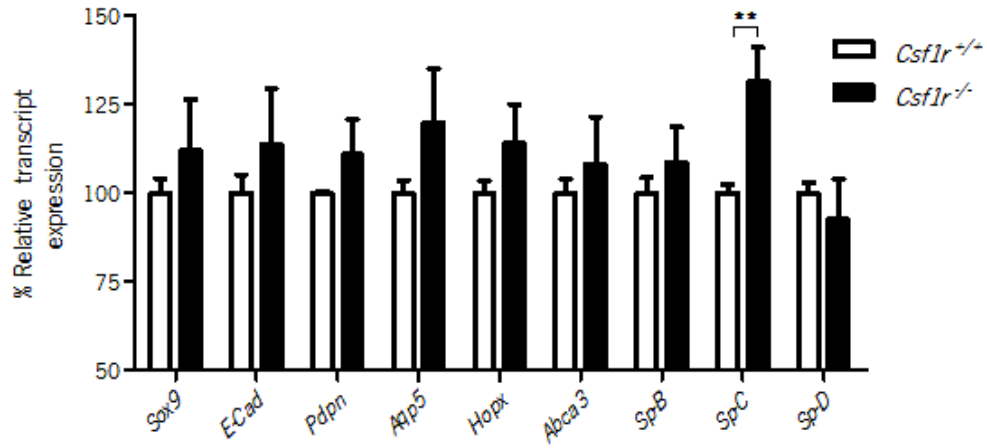


Figure 5- Distal epithelium transcripts expression analysis at canalicular stage (E16.5).

Distal progenitor cell (*Sox9*), epithelium (*E-cad*) and alveolar epithelium (*Pdpn*, *Aqp5*, *Hopx*, *Abca3*, *Sp-B*, *Sp-C* and *Sp-D*) transcripts were assessed in *Csf1r*^{-/-} and *Csf1r*^{+/+} lungs by qPCR. *Gapdh* transcript expression was used as housekeeping gene. (*p < 0.05, **p < 0.01 and ***p < 0.0001)

In the same group, AT1 related transcripts demonstrated a 35-50% augment in *Csf1r*^{-/-} lungs (*Pdpn* (37%): 136.8±5.10 (N=7) vs 100.0±0.48 (N=10), p<0.0001; *Hopx* (41%): 140.6±8.53 (N=7) vs 100.0±3.52 (N=10), p=0.0002 and *Aqp5* (50%): 150.3±18.10 (N=7) vs 100.0±3.62 (N=11), p=0.0039) and AT2 markers a 25-65% increase (*Abca3* (64%): 163.6±10.48 (N=4) vs 100.0±4.04 (N=11), p<0.0001; *Sp-B* (33%): 133.1±7.60 (N=7) vs 100.0±4.44 (N=11), p=0.0009 and *Sp-D* (26%): 125.6±8.09 (N=5) vs 100.0±2.98 (N=10), p=0.0028) (Figure 6B). In *Csf1r*^{-/-} down sub-group, *Sox9* and *E-cad* were 26% decrease (74.5±4.20 (N=6) vs 100.0±4.23 (N=10), p=0.0013; 73.6±6.22 (N=6) vs 100.0±5.20 (N=11), p=0.0069, respectively) (Figure 6B). AT1 transcripts presented a reduction of 20-30% in expression levels (*Pdpn* (25%): 74.7±6.43 (N=5) vs 100.0±0.48 (N=10), p<0.0001; *Aqp5* (23%): 77.5±8.06 (N=5) vs 100.0±3.62 (N=11), p=0.0099 and *Hopx* (23%): 77.1±6.87 (N=5) vs 100.0±3.52 (N=10), p=0.0055) and AT2 transcripts were 25-35% diminish (*Abca3* (34%): 65.7±5.68 (N=5) vs 100.0±4.04 (N=11), p=0.0003; *Sp-B* (26%): 74.2±7.24 (N=5) vs 100.0±4.44 (N=11), p=0.0070 and *Sp-D* (35%): 65.0±9.70 (6) vs 100.0±2.97 (10), p=0.0009) (Figure 6B).

A



B

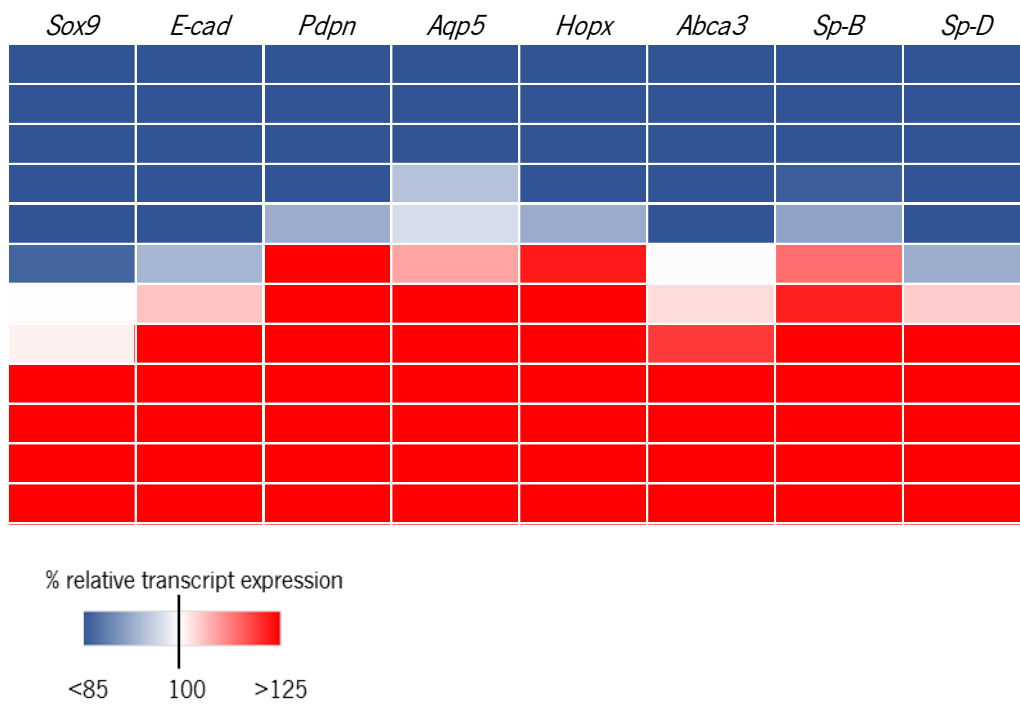


Figure 6- Distal epithelium transcripts expression analysis at saccular stage (E18.5).

(A) Distal progenitor cell (*Sox9*), epithelium (*E-cad*) and alveolar epithelium (*Pdpn*, *Aqp5*, *Hopx*, *Abca3*, *Sp-B*, *Sp-C* and *Sp-D*) transcripts were assessed in *Csf1r*^{-/-} and *Csf1r*^{+/+} lungs by qPCR. (B) Heatmap representation of distal epithelium related transcripts differentially expressed in *Csf1r*^{-/-} lungs compared with *Csf1r*^{+/+} demonstrating two distinctive expression patterns (*Csf1r*^{-/-} up (red) and down (blue)). *Gapdh* transcript expression was used as housekeeping gene. (*p < 0.05, **p < 0.01 and ***p < 0.0001)

Our unpublished data showed lung morphological impairments at this lung developmental stage but also at postnatal saccular stage. To understand whether alveolar differentiation state of newborn (P0) *Csf1r*^{-/-} is disturbed, we performed a similar quantitative analysis of the relative transcript levels at this time point (Figure 7). Distal epithelium transcript analysis demonstrated statistical and higher increase in *Sox9* of 148% (247.8±66.70 vs 100.0±4.58, p=0.0240) and *E-cad* of 28% (127.5±10.52 vs 100.0±3.43, p=0.0120) (Figure 7). Most of AT1 transcripts were augmented in *Csf1r*^{-/-} lungs (*Aqp5* (31%): 130.9±9.58 vs 100.0±7.61, p=0.0228 and *Hopx* (41%): 140.6±19.73 vs 100.0±1.83, p=0.0464) (Figure 7). *Pdpr* transcript had distinct expression levels (*Csf1r*^{-/-} up 24% increased; 123.6±15.44 (N=4) vs 100.0±0.496 (N=8), p=0.0463; and *Csf1r*^{-/-} down 25% decreased (75.08±6.28 (N=3) vs 100.0±0.496 (N=8), p<0.0001). Towards AT2 related transcripts, only *Abca3* transcript expression was changed with an increase of 31% (131.0±13.76 vs 100.0±4.80, p=0.0278) (Figure 7).

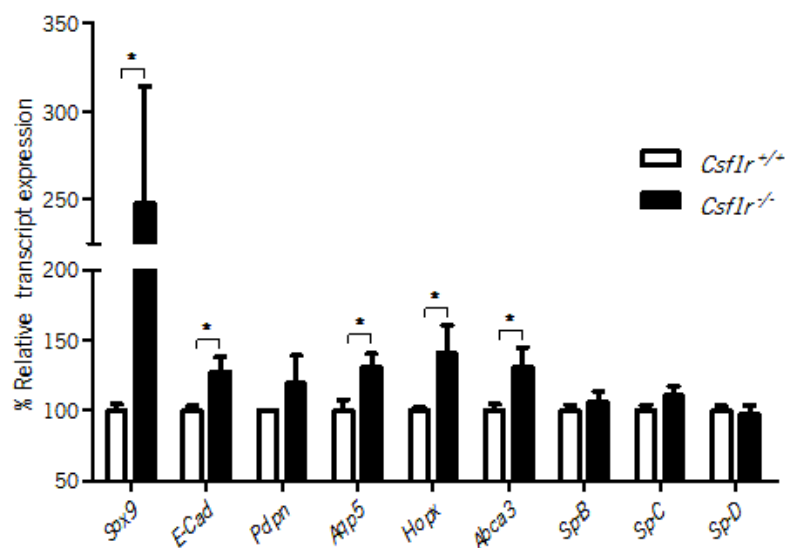


Figure 7- Distal epithelium transcripts expression analysis at saccular stage (P0).

(A) Distal progenitor cell (*Sox9*), epithelium (*E-cad*) and alveolar epithelium (*Pdpr*, *Aqp5*, *Hopx*, *Abca3*, *Sp-B*, *Sp-C* and *Sp-D*) transcripts were assessed in *Csf1r*^{-/-} and *Csf1r*^{+/+} lungs by qPCR. *Gapdh* transcript expression was used as housekeeping gene. (*p < 0.05, **p < 0.01 and ***p < 0.0001)

Accordingly, qPCR analysis of E18.5 showed a clear dysregulation in distal epithelium transcripts expression in *Csf1r*^{-/-} lungs. This phenomenon seemed to begin at E16.5, and it was maintained during saccular stage in *Csf1r*^{-/-} newborns (P0). Although, AT2 transcripts seemed to present a recovery in the expression levels, AT1 transcripts maintained a dysregulated expression in *Csf1r*^{-/-} lungs. Altogether these results suggest that absence of tissue macrophages promote a clear dysregulation in the transcript levels of most distal epithelial markers studied, and consequently point out a possible failure in alveolar differentiation in *Csf1r*^{-/-} mice during lung formation.

To assess if the alveolar differentiation was disturbed at E18.5, AT1 and AT2 markers expression, Aqp5 and Sp-C respectively, was investigated by immunofluorescence staining. A first observational analysis suggested decreased Aqp5 and proSp-C expression levels in *Csf1r*^{-/-} mice (Figure 8A).

Both Aqp5 and proSp-C proteins expression area was 22% reduced in *Csf1r*^{-/-} lungs (0.0349 ± 0.00448 vs 0.0449 ± 0.00127 , $p=0.0395$ and 0.0668 ± 0.00462 vs 0.0856 ± 0.00339 , $p=0.0044$, respectively) (Figure 8B). This result confirmed that distal epithelium differentiation is disrupted in tissue macrophage-deficient lungs, as suggested by qPCR results.

To confirm if the alveolar differentiation impairments visualized in early saccular stage is also present in newborn *Csf1r*^{-/-} mice, we evaluated AT1 and AT2 markers protein expression at P0. Observational analysis suggested a decrease in Aqp5 expression, and no effect on proSp-C protein expression in *Csf1r*^{-/-} lungs (Figure 9A). At P0, proSp-C protein expression area quantification showed no differences in *Csf1r*^{-/-} lungs (0.1048 ± 0.00887 vs 0.0943 ± 0.00385 , $p=0.2300$) (Figure 9B). On the other hand, Aqp5 protein expression exhibited a significantly decrease (18%) in AT1 cell marker (0.0851 ± 0.00539 vs 0.1032 ± 0.00367 , $p=0.0112$) (Figure 9B). Impairments in the alveolar differentiation were corroborated in both transcript and protein expression analysis performed in *Csf1r*^{-/-} lungs, indicating *Csf1r*-positive macrophages as key players in the regulation of alveolar differentiation during saccular stage.

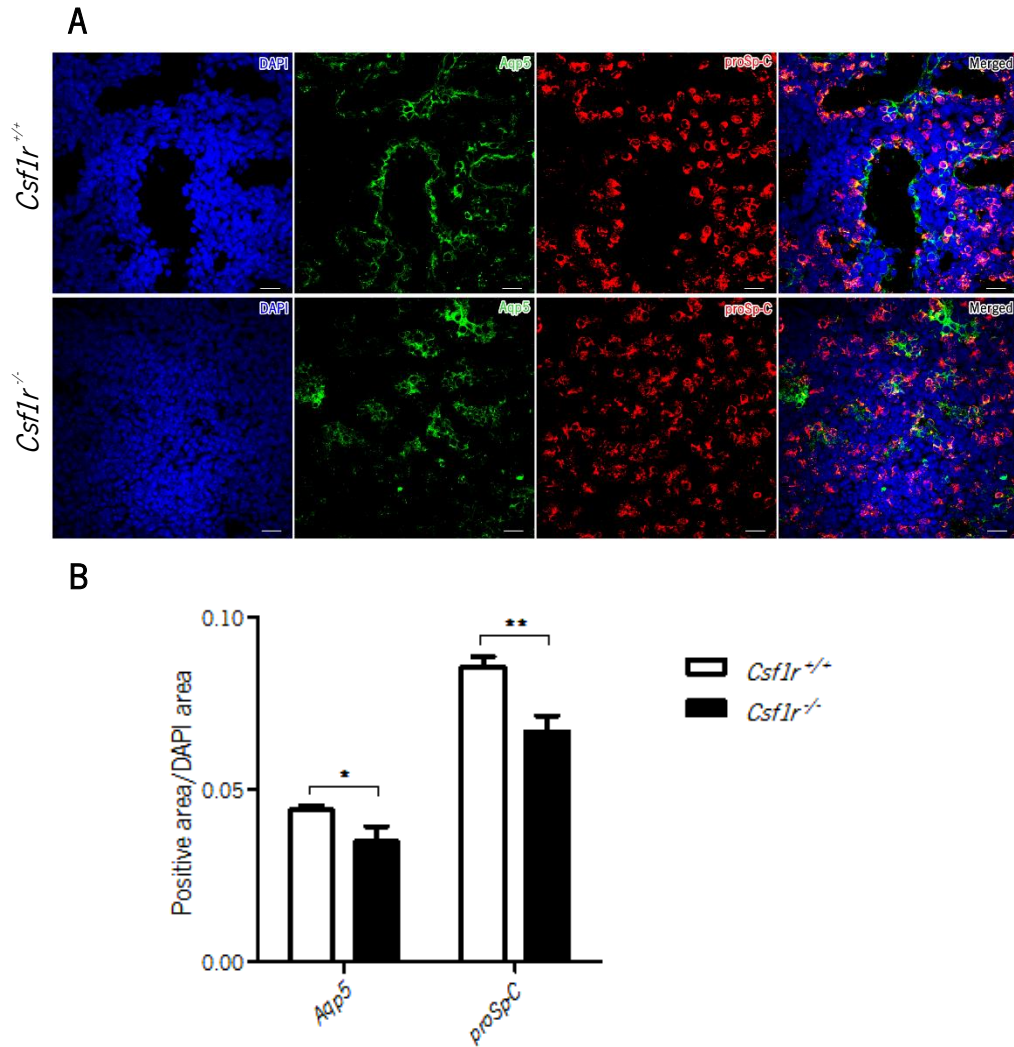


Figure 8- Aqp5 and proSp-C expression in *Csfl1r*^{-/-} lungs at saccular stage (E18.5).

(A) Representative images (60x) of Aqp5 (green) and proSp-C (red) protein expression pattern in *Csfl1r*^{-/-} in comparison with *Csfl1r*^{+/-} lungs by immunofluorescence. Nuclear staining was performed using DAPI (blue).

(B) Quantification of Aqp5 and proSp-C positive expression areas per lung parenchyma area (DAPI positive area). (* $p < 0.05$, ** $p < 0.01$ and *** $p < 0.0001$)

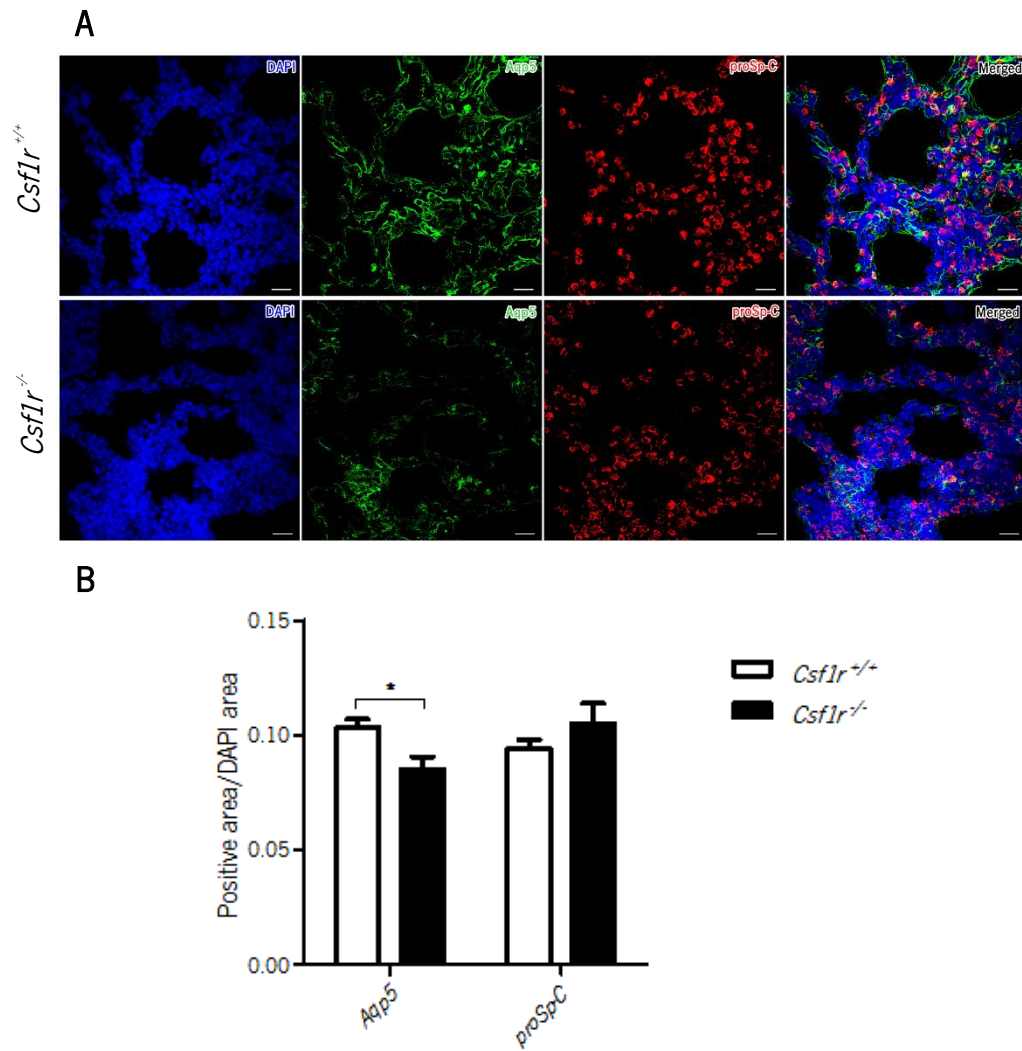


Figure 9- Aqp5 and proSp-C expression in *Csf1r*^{-/-} lungs at saccular stage (P0).

(A) Representative images (60x) of Aqp5 (green) and proSp-C (red) protein expression pattern in *Csf1r*^{-/-} in comparison with *Csf1r*^{+/+} lungs by immunofluorescence. Nuclear staining was performed using DAPI (blue).

(B) Quantification of Aqp5 and proSp-C positive expression areas per lung parenchyma area (DAPI positive area). (*p < 0.05, **p < 0.01 and ***p < 0.0001)

4.2 Tissue macrophages modulation of bronchiole differentiation

During pseudoglandular stage (E11.5-16.5) occurs epithelial conducting tubes division, a process called branching morphogenesis¹⁶. During this process occurs bronchi, bronchioles and alveoli formation. Bronchi and bronchioles are constituted by Clara cells, basal cells, ciliated cells, neuroendocrine cells, goblet cells, smooth muscle cells and others⁷. Morphological analysis in *Csf1r*^{-/-} lungs at saccular stage (E18.5 and P0) did not present differences in bronchiole-like structures. However, *E-cad* expression was already assessed in alveolar epithelium analyses and showed dysregulation in transcript expression during canalicular and saccular stage, indicating that lung epithelium was affected in *Csf1r*^{-/-} lungs. So, to confirm if the proximal conducting airways epithelial differentiation were correctly developed in *Csf1r*^{-/-} lungs, transcript expression analysis was assessed throughout lung development (E16.5, E18.5 and P0 lungs). To assess proximal epithelium differentiation, we quantified *Sox2* (proximal progenitor cells), *Foxj1* (ciliated cells), *Scgb1a1* (Clara cells) and *Calca* (neuroendocrine cells) transcript levels by qPCR.

Sox2 and *Scgb1a1* expression were not changed in *Csf1r*^{-/-} lungs at E16.5 (110.5±7.73 vs 100.0±4.39, p=0.2152 and 116.8±15.24 vs 100.0±6.99, p=0.2641). *Foxj1* and *Calca* transcripts, ciliated and neuroendocrine cell markers respectively, were statistically increased, 31% (131.4±15.59 vs 100.0±3.42, p=0.0442 and 130.6±10.88 vs 100.0±3.92, p=0.0071; respectively) (Figure 10).

At E18.5, *Calca* was highly increased (69%) in *Csf1r*^{-/-} (169.4±18.00 vs 100.0±3.42, p=0.0018) (Figure 11A). On the other hand, *Sox2*, *Scgb1a1* and *Foxj1* presented a heterogeneous expression patterns (Figure 11B). In *Csf1r*^{-/-} up sub-group, *Sox2* expression was 33% increase (133.7±7.60 (N=7) vs 100.0±4.44 (N=11), p=0.0009), *Scgb1a1* expression increased 43% (143.0±9.81 (N=6) vs 100.0±4.93 (N=11), p=0.0002) and *Foxj1* 25% (124.4±4.30 (N=5) vs 100.0±3.62 (N=11), p=0.0014) (Figure 11B). In *Csf1r*^{-/-} down sub-group *Sox2* expression was 26% decreased (74.2±7.24 (N=5) vs 100.0±4.44 (N=11), p=0.0070), *Scgb1a1* expression decreased 36% (64.3±11.40 (N=5) vs 100.0±4.93 (N=11), p=0.0042). *Foxj1* expression was decreased but without statistical difference (89.1±3.56 (N=6) vs 100.0±3.62 (N=11), p= 0.0704) (Figure 11B).

Newborn (P0) *Csf1r*^{-/-} lungs did not present differences in *Sox2* expression (100.0±6.77 vs 105.7±7.94, p=0.5919) and *Scgb1a1* expression (121.3±10.93 vs 100.0±4.64, p=0.0708) (Figure 12). *Foxj1* transcripts levels were statistical 17% increase (116.8±7.98 vs 100.0±1.66, p=0.0262) (Figure 12). *Calca* expression levels exhibited a *Csf1r*^{-/-} up sub-group with 32% increase (100.0±3.48 (N=9) vs 132.0±7.29 (N=4), p=0.0008) and a *Csf1r*^{-/-} *Csf1r*^{+/-}-like sub-group (100.0±3.48 (N=9) vs 93.60±2.71 (N=4), p=0.2783). These results show a possible dysregulation in bronchiole transcripts expression, although no morphological changes were observed in this lung epithelial compartment due to tissue macrophages.

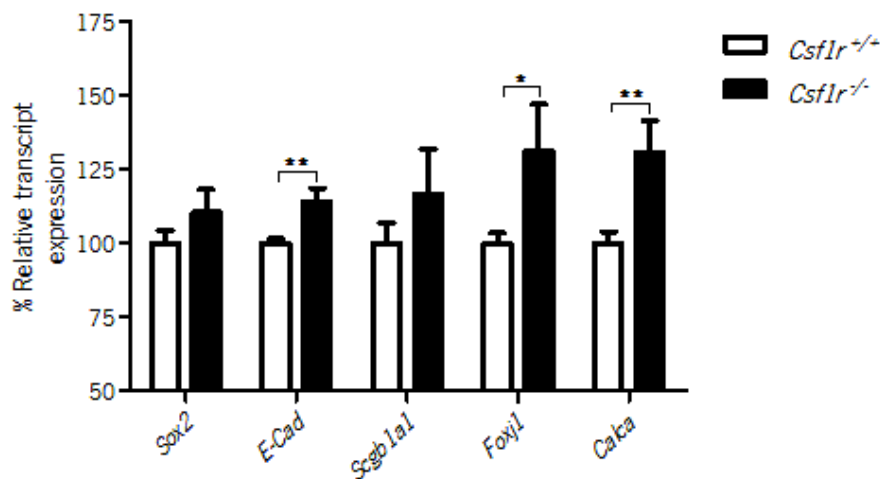


Figure 10- Proximal epithelium transcripts expression analysis at canalicular stage (E16.5).

(A) Proximal progenitor cell (*Sox2*), epithelium (*E-cad*) and proximal epithelium markers (*Scgb1a1*, *Foxj1* and *Calca*) transcripts levels were assessed in *Csf1r*^{+/-} and *Csf1r*^{-/-} lungs by qPCR. *Gapdh* transcript expression was used as housekeeping gene. (*p < 0.05, **p < 0.01 and ***p < 0.0001).

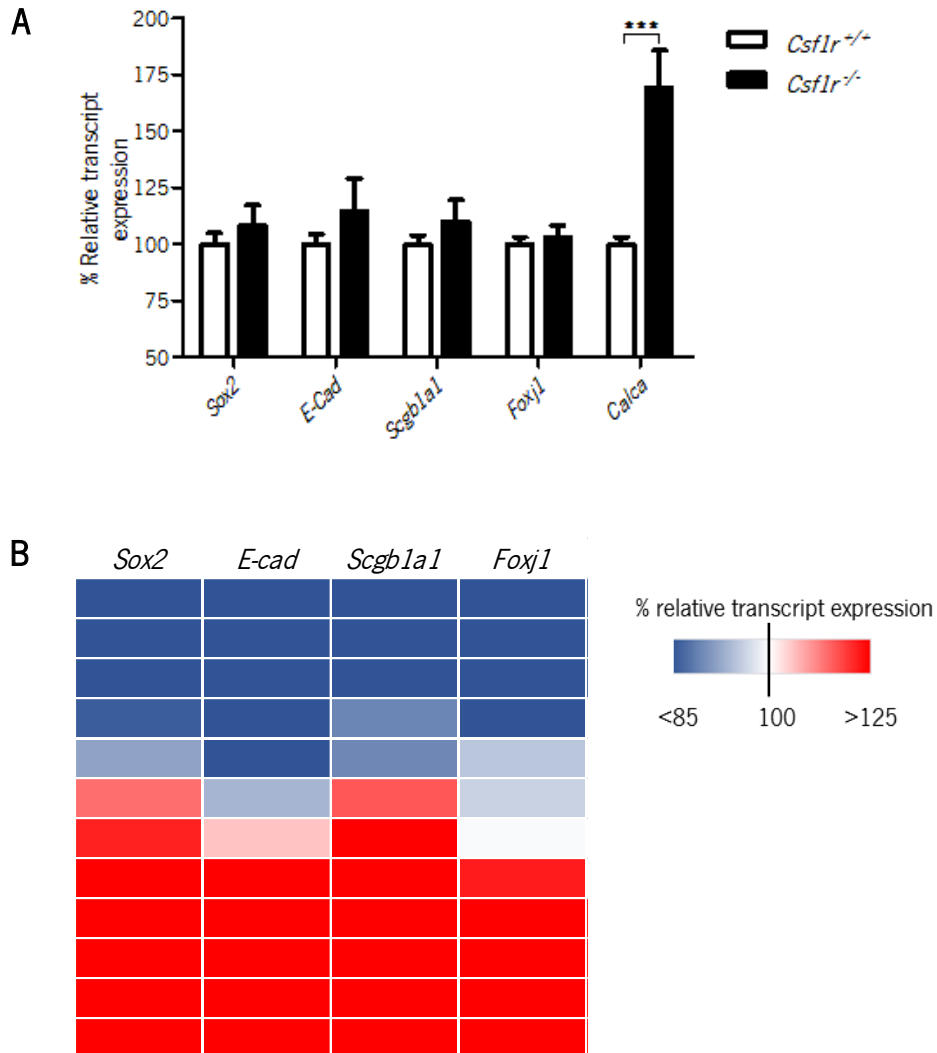


Figure 11- Proximal epithelium transcripts expression analysis at early saccular stage (E18.5).

(A) Progenitor cell (*Sox2*), epithelium (*E-cad*) and proximal epithelium markers (*Scgb1a1*, *Foxj1* and *Calca*) transcripts levels were assessed in *Csf1r*^{+/+} and *Csf1r*^{-/-} lungs by qPCR. (B) Heatmap representation of proximal epithelium related transcripts, demonstrating two distinctive expression patterns (*Csf1r*^{-/-} up (red) and down (blue)). *Gapdh* transcript expression was used as housekeeping gene. (*p < 0.05, **p < 0.01 and ***p < 0.0001)

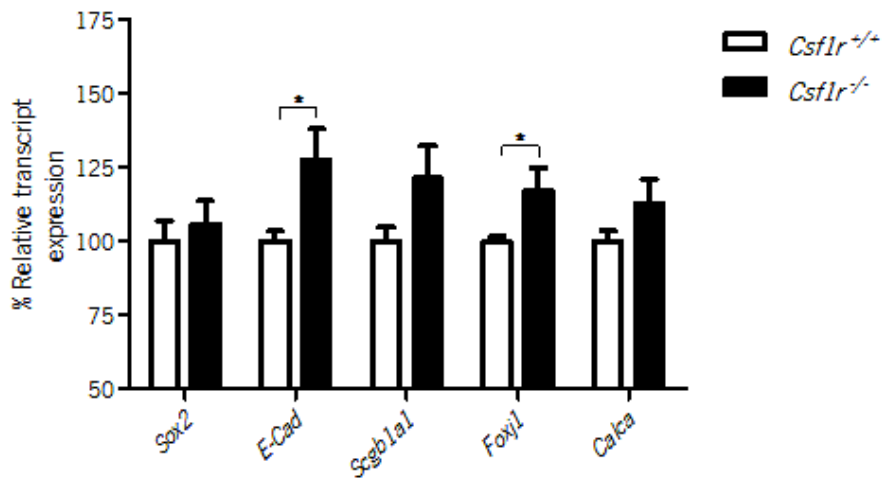


Figure 12- Proximal epithelium transcripts expression analysis at saccular stage (P0).

(A) Proximal progenitor cell (*Sox2*), epithelium (*E-cad*) and proximal markers (*Scgb1a1*, *Foxj1* and *Calca*) transcripts were assessed in *Csf1r*^{+/+} and *Csf1r*^{-/-} lungs by qPCR. *Gapdh* transcript expression was used as housekeeping gene. (*p < 0.05, **p < 0.01 and ***p < 0.0001)

4.3 Impact of tissue macrophages in lung vasculature formation

So far, morphological, transcription and protein analysis revealed that tissue macrophages are involved in alveolar and suggested a possible dysregulation on bronchiole differentiation during lung development. However, it is unknown if tissue macrophages are involved in vasculature formation during lung development.

Vasculature development starts during the beginning of pseudoglandular stage and develops concomitantly with branching morphogenesis^{19,20}. Moreover, epithelial cells produce growth factors essentials to vasculature formation and maturation, such as *Vegfa*²⁸, indicating a obviously interaction between epithelial and endothelial morphogenesis. Interestingly in hindbrain, macrophages are indicated as modulators of vascular anastomoses formation⁴⁶. Taking these evidences in consideration an obvious question arises: it is vascular compartment firstly affected and, consequently occur an impairment in epithelium formation or alveolar impairments induce vascular defects during lung development. To investigate these, we evaluated vasculature formation through quantification of vascular mediators' transcripts relative expression and endothelial protein cell markers by qPCR at E16.5, E18.5 and P0. On this way, we expect to understand which of the systems is firstly affected by tissue macrophages absence, but also when it occurs.

At E16.5, most of the vascular mediators' transcripts expression levels in *Csf1r*^{-/-} lungs did not show statistical differences in comparison with *Csf1r*^{+/-} lungs, except *Hif-1α* and *Ang-1*. These two transcripts were slightly increased, 8-10% (*Hif-1α*: 107.5±3.27 vs 100.0±1.36 and *Ang1*: 109.8± 3.87 vs 100.0±1.98, p=0.0234) (Figure 13).

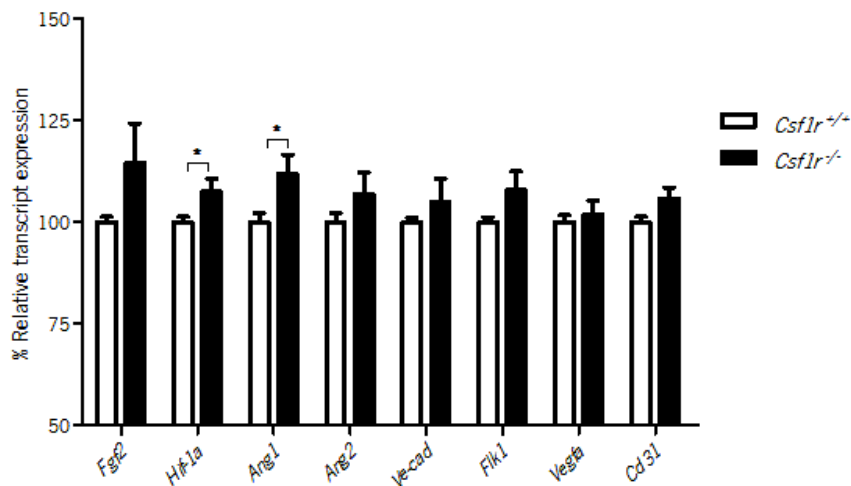


Figure 13- Vascular mediators' transcripts expression analysis at canalicular stage (E16.5).

Vascular mediators' transcripts were assessed in *Csf1r*^{+/-} and *Csf1r*^{-/-} lungs by qPCR. *Gapdh* transcript expression was used as housekeeping gene. (*p < 0.05, **p < 0.01 and ***p < 0.0001)

In early saccular stage, E18.5, it was possible to observed a significantly decrease of 21% in *Fgf2* expression (79.0±3.56 vs 100.0±1.50, p<0.0001) (Figure 14A). Moreover, a detailed analysis demonstrated the distinction of two *Csf1r*^{-/-} sub-groups (*Csf1r*^{-/-} up and *Csf1r*^{-/-} down, as already identified in epithelial analysis) in some vascular mediators: *Ve-cad*, *Flk1*, *Vegfa* and *Cd31*. In *Csf1r*^{-/-} up sub-group of mice a 30-50% increase was showed (*Ve-cad* 40%, 140.0±9.20 (N=7) vs 100.0±5.03 (N=11), p=0.0007); *Flk1* 48% (147.9±9.83 (N=5) vs 100.0±4.18 (N=11), p=0.0001); *Vegfa* 33% (132.9±10.86 (N=6) vs 100.0±3.52 (N=11), p=0.0027); *Cd31* 39% (139.2±10.95 (N=7) vs 100.0±2.57 (N=10), p=0.0009) (Figure 14B). In *Csf1r*^{-/-} down lungs, *Ve-cad* was 33% decreased (67.5±7.09 (N=5) vs 100.0±5.03 (N=11), p=0.0025), *Flk1* was 38% (62.3±7.35 (N=5) vs 100.0±4.18 (N=11), p=0.0003), *Vegfa* was 15% (85.1±5.80 (N=5) vs 100.0±3.52 (N=11), p=0.0383) and *Cd31* was 22% decreased (77.8±8.09 (N=5) vs 100.0±2.57 (N=10), p=0.0052) (Figure 14B).

At P0, *Csf1r*^{-/-} lungs showed impairments in the transcript expression of *Ang2*, *Hif-1α* and *Flk1*. In specific, a decrease of 17% in *Ang2* expression (82.6 ± 6.80 vs 100.0 ± 2.84 , $p=0.0218$), increase of 15% in *Hif-1α* (114.7 ± 6.69 vs 100.0 ± 1.76 , $p=0.0317$) and 19% increase in *Flk1* expression (119.2 ± 5.58 vs 100.0 ± 4.62 , $p=0.0182$) (Figure 15A). A more detailed analysis concerning the presence of *Csf1r*^{-/-} sub-groups showed changes in *Ang1* expression: *Csf1r*^{-/-} up with 21% increase (121.1 ± 3.11 (N=4) vs 100.0 ± 3.41 (N=10), $p=0.0035$) and *Csf1r*^{-/-} down 32% decrease (68.0 ± 5.84 (N=3) vs 100.0 ± 3.41 (N=10), $p=0.0008$). *Ang2* expression exhibited a 34% decrease (66.1 ± 4.24 (N=4) vs 100.0 ± 2.84 (N=10), $p < 0.0001$) in a half of *Csf1r*^{-/-} lungs (*Csf1r*^{-/-} down) and the other half presented similar expression levels to *Csf1r*^{+/+} lungs (99.2 ± 3.92 (N=4) vs 100.0 ± 2.84 (N=10), $p=0.8785$) (Figure 15B). *Vegfa* expression was 72% increase in majority of *Csf1r*^{-/-} up sub-group (172.2 ± 25.22 (N=5) vs 100.0 ± 2.79 (N=8), $p=0.0038$) and the others *Csf1r*^{-/-} mice showed expression levels like *Csf1r*^{+/+} lungs (95.0 ± 1.37 (N=3) vs 100.0 ± 2.79 (N=8), $p=0.3226$) (Figure 15B). Shortly, dysregulation of vascular mediators' transcript expression by tissue macrophages was evident only at sacular stage (E18.5).

To assess whether these transcript expression impairments is traduced in a change in the vasculature formation morphology, IF staining was performed to specific endothelial markers, Ve-cad and Cd31 at E18.5 and P0 (Figures 16A and 17A). At early sacular stage E18.5, Ve-cad marker did not present statistical differences between *Csf1r*^{+/+} and *Csf1r*^{-/-} lungs (0.1129 ± 0.00646 vs 0.1103 ± 0.00400 , $p=0.7324$) (Figure 16B). Cd31 marker in *Csf1r*^{-/-} mice was decreased in 12% (0.0890 ± 0.00479 vs 0.1011 ± 0.00294 , $p=0.0337$) (Figure 16B).

At P0, Ve-cad and Cd31 markers showed a 22 and 27% decreased expression (0.1743 ± 0.01546 vs 0.2229 ± 0.01295 , $p=0.0323$ and 0.828 ± 0.01814 vs 0.2502 ± 0.01728 , $p=0.0218$, respectively) (Figure 17B). Impairments in vasculature maturation were corroborated in both transcript and protein expression analysis performed in *Csf1r*^{-/-} lungs.

Taking in consideration the influence of alveolar epithelium during vasculature differentiation, we cannot suggest that the vascular formation defects was a direct consequence of tissue macrophages absence, because alveolar compartment was firstly affected as transcript analysis at canalicular phase suggests. So, disruption of vasculature formation at sacular stage could be a consequence of alveolar differentiation dysregulation and not directly a consequence of tissue macrophages absence.

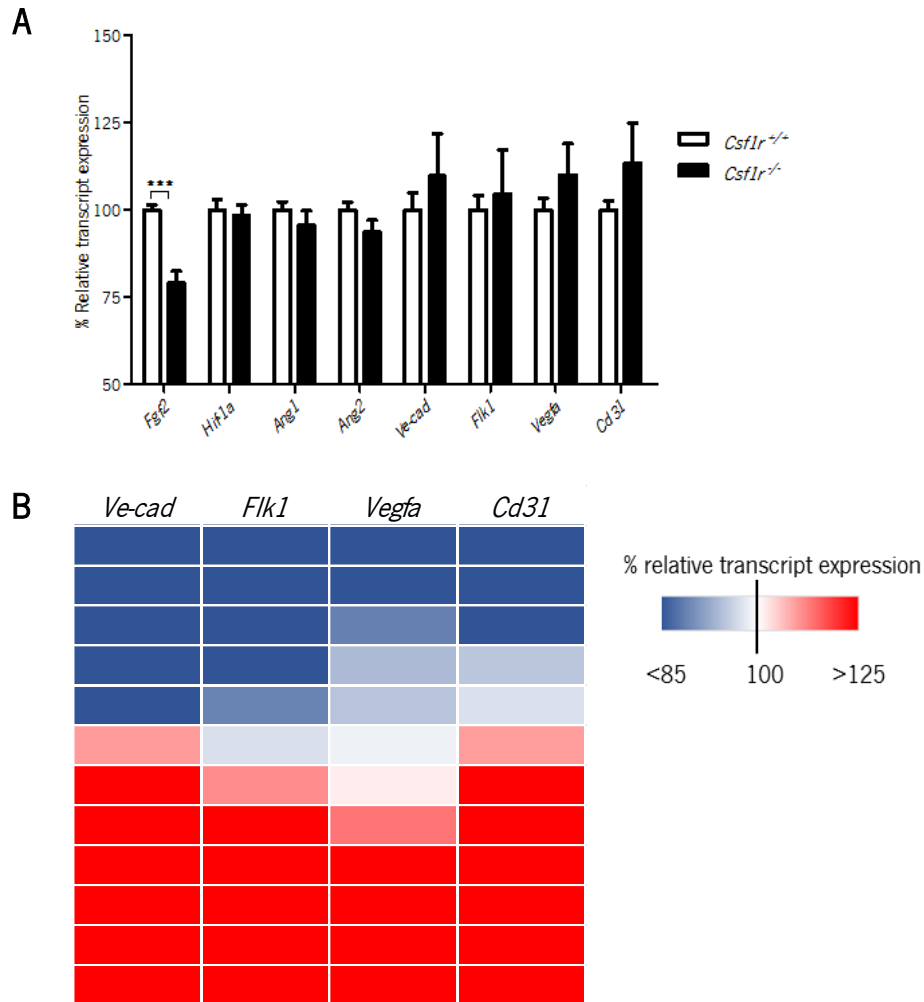
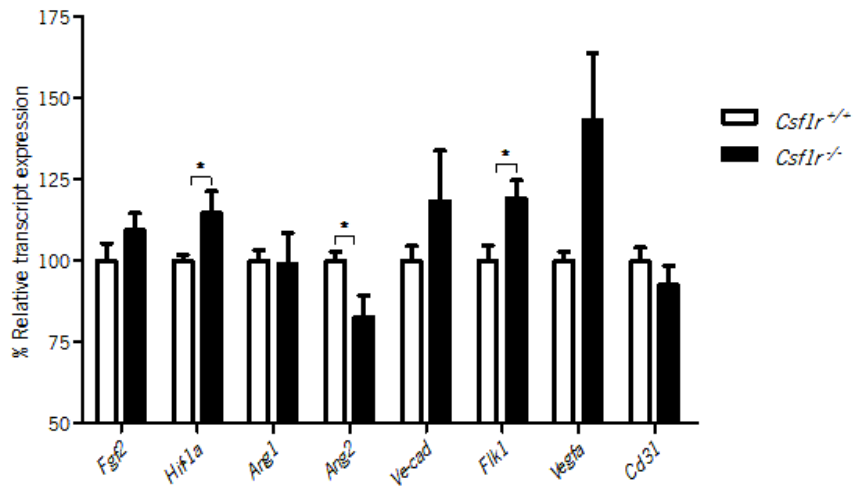


Figure 14- Vascular mediators' transcripts expression analysis at early saccular stage (E18.5).

(A) Vascular mediators' transcripts were assessed in *Csflr*^{+/+} and *Csflr*^{-/-} lungs by qPCR. (B) Heatmap representation of vascular mediators related transcripts, demonstrating two distinctive expression patterns (*Csflr*^{-/-} up (red) and down (blue)). *Gapdh* transcript expression was used as housekeeping gene. (*p < 0.05, **p < 0.01 and ***p < 0.0001)

A



B

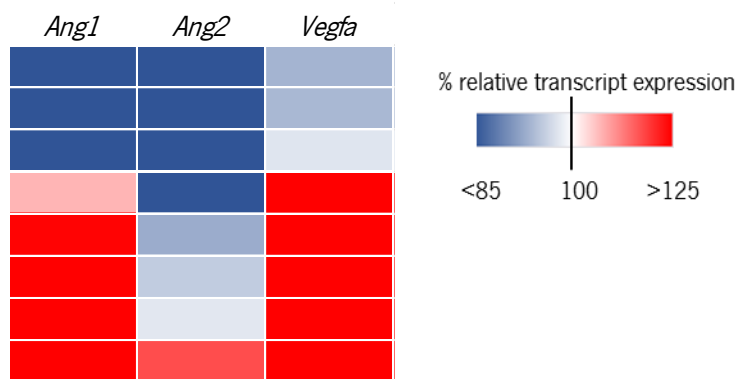


Figure 15- Vascular mediators' transcripts expression analysis at saccular stage (P0).

(A) Vascular mediators' transcripts were assessed in *Csf1r*^{-/-} and *Csf1r*^{+/+} lungs by qPCR. (B) Heatmap representation of vascular mediators related transcripts, demonstrating two distinctive expression patterns (*Csf1r*^{-/-} up (red) and down (blue)). *Gapdh* transcript expression was used as housekeeping gene. (*p < 0.05, **p < 0.01 and ***p < 0.0001)

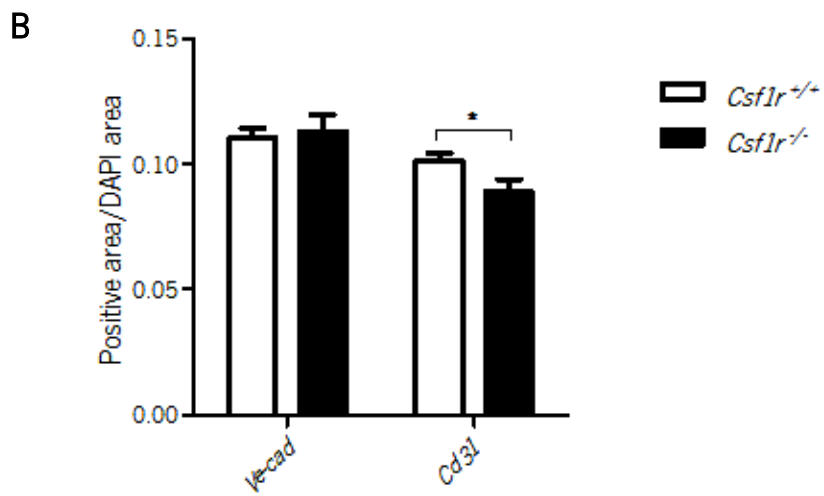
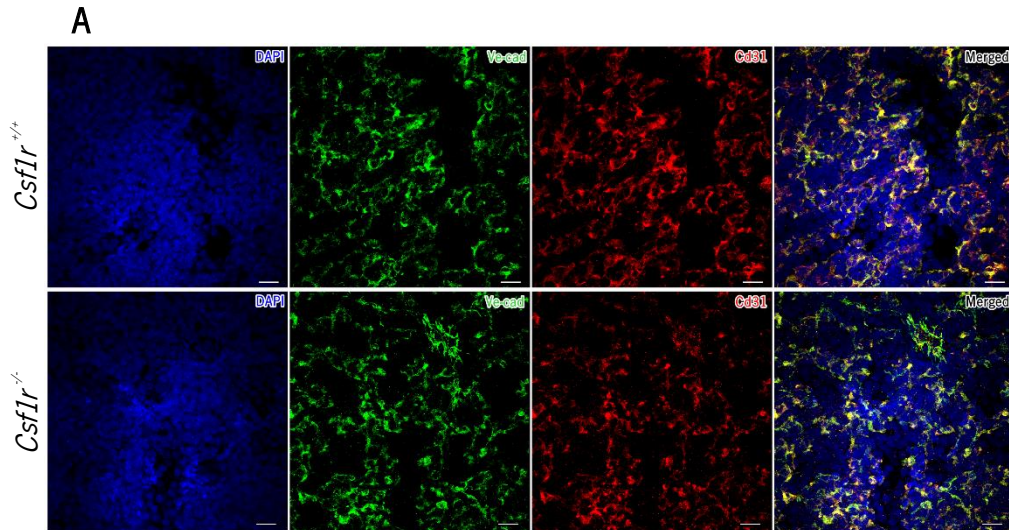


Figure 16- Ve-cad and Cd31 expression in *Csf1r*^{-/-} lungs at early saccular stage (E18.5).

(A) Representative images (60x) of Ve-cad (green) and Cd31 (red) protein expression pattern in *Csf1r*^{-/-} in comparison with *Csf1r*^{+/+} lungs by immunofluorescence. Nuclear staining was performed using DAPI (blue).

(B) Quantification of Ve-cad and Cd31 positive expression areas per lung parenchyma area (DAPI positive area). (*p < 0.05, **p < 0.01 and ***p < 0.0001)

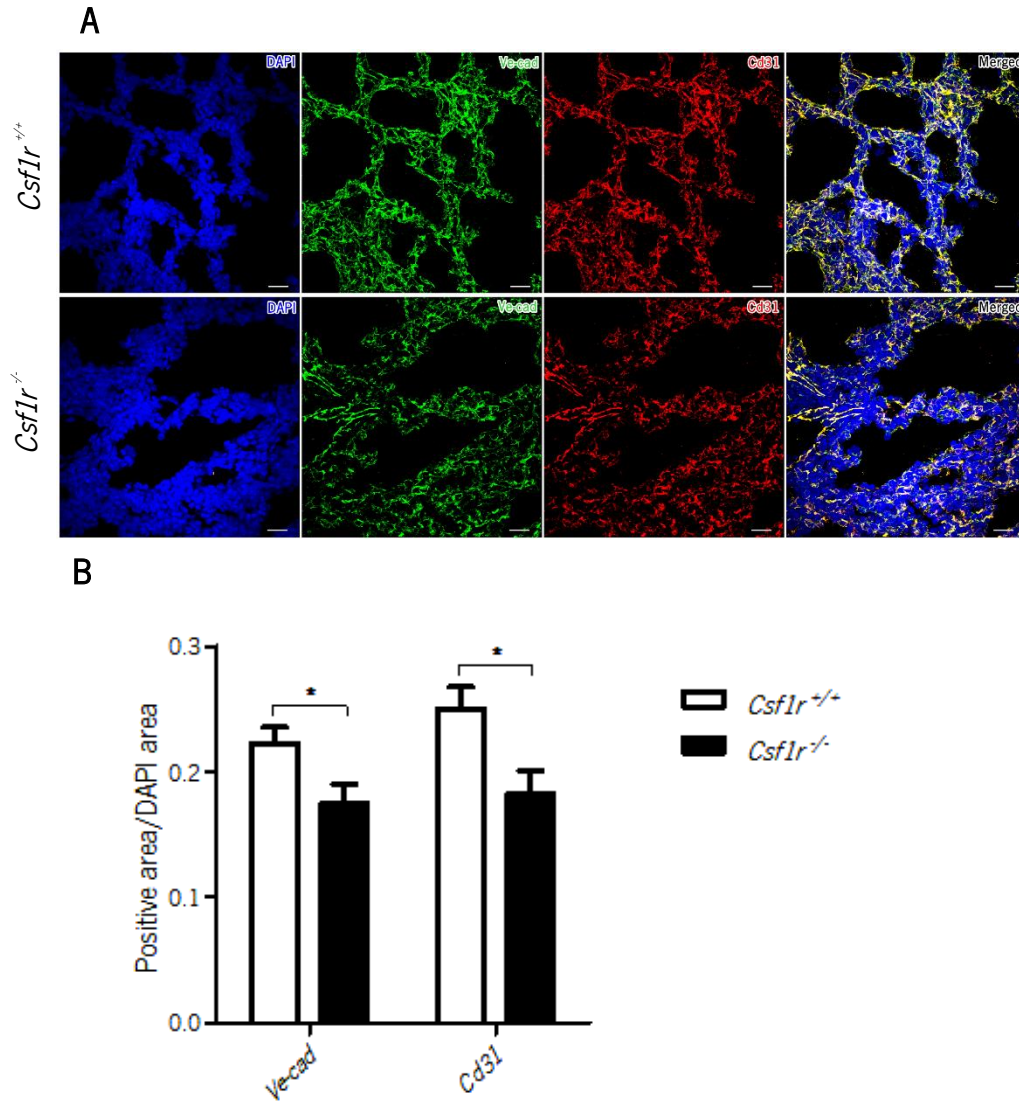


Figure 17- Ve-cad and Cd31 expression in *Csf1r*^{-/-} lungs at early saccular stage (P0).

(A) Representative images (60x) of Ve-cad (green) and Cd31 (red) protein expression pattern in *Csf1r*^{+/+} in comparison with *Csf1r*^{-/-} lungs by immunofluorescence. Nuclear staining was performed using DAPI (blue).

(B) Quantification of Ve-cad and Cd31 positive expression areas per lung parenchyma area (DAPI positive area). (*p < 0.05, **p < 0.01 and ***p < 0.0001)

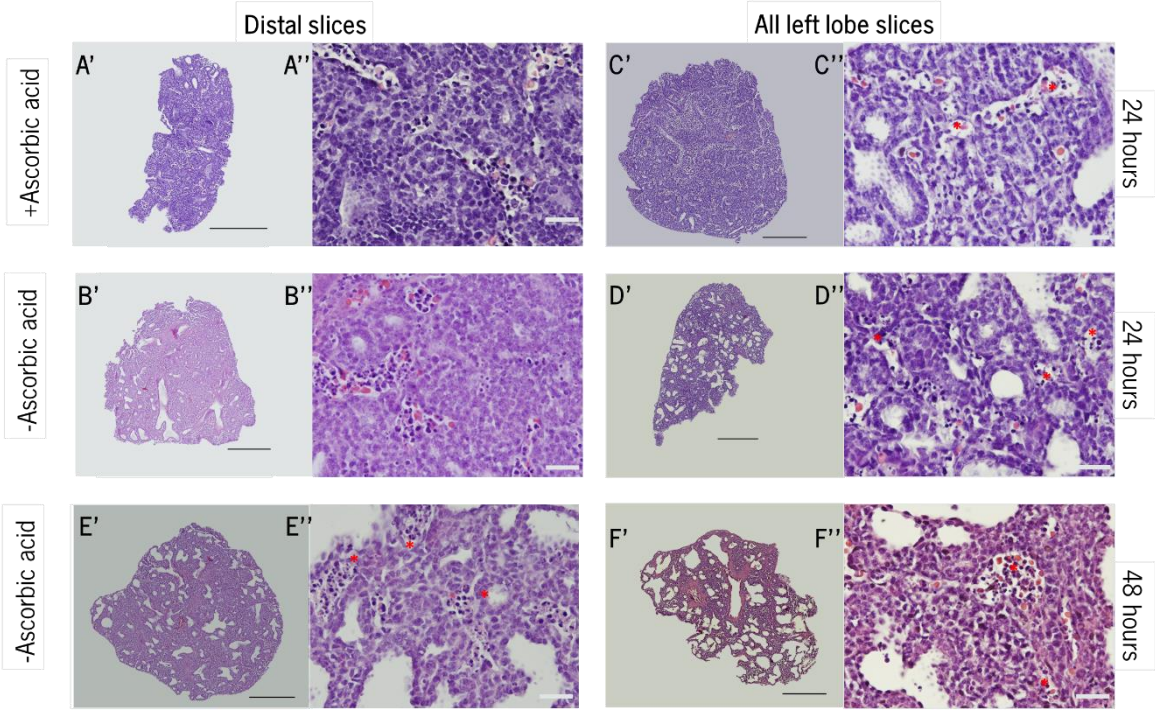
4.4 Establishment of E16.5 lung slices in culture

A commonly culture technique used to perform functional assays to study cellular and molecular processes during lung saccular developmental stage, such as alveolar differentiation or vasculature formation, is the culture of lung explants, the also called lung slice cultures. Different approaches have been applied in the culture optimization such as left lobe region of cut or ascorbic acid supplementation^{34,65,66}. Ascorbic acid, also known as vitamin C, is an antioxidant and can scavenge free radicals, protecting cells from oxidative damage⁶⁷, and it has been associated with increase in viability of tissue culture. Since we intend to validate that tissue macrophages are involved in alveolar differentiation and/or vasculature formation, we decided to optimize lung slice culture to perform the inhibition of Csf1r-positive macrophages and evaluate lung morphology, and consequently assess alveolar and vasculature formation.

In this work, we intend to optimize the best conditions to decrease tissue death on lung slices culture. Different conditions were considered: culture of different lung regions and culture in medium supplemented with ascorbic acid. Different lung regions were tested to understand if different left lobe areas (proximal or distal areas) were more viable in culture and if ascorbic acid supplementation increase lung slices survival. To assess viability, we quantified apoptotic bodies areas in lung slices H&E stained.

Lung slices performed in the distal area did not demonstrate differences in tissue viability between the culture medium with (Figure 18A) or without ascorbic acid during 24 hours (Figure 18B) (0.115 ± 0.0158 vs 0.105 ± 0.0159 , $p=0.7017$) (Figure 18G). However, when all lung cuts were cultured in supplemented (Figure 18C) and non-supplemented (Figure 18D) medium, non-ascorbic acid supplementation showed a statistical 42% decrease in apoptotic bodies areas in comparison with ascorbic acid supplementation (0.190 ± 0.0247 vs 0.111 ± 0.0158 , $p=0.0351$) (Figure 18D). Furthermore, we compared distal and all left lobe slices with and without ascorbic acid supplementation to understand if lung zone could influence lung culture viability. All left lobe slices showed no differences in apoptotic bodies when compared to distal slices, both with ascorbic acid supplementation (0.190 ± 0.0247 vs 0.115 ± 0.0158 , $p=0.0654$) (Figure 18G). In non-ascorbic acid supplementation, no differences were seen in apoptotic bodies areas between distal and all left lobe slices (0.105 ± 0.0159 vs 0.111 ± 0.0158 , $p=0.8102$). Additionally, we performed distal (Figure 18E) and all left lobe slices (Figure 18F) culture without medium supplementation during 48 hours. Apoptotic bodies areas were quantified and no statistical differences were seen in comparison with the same conditions at 24 hours (distal: 0.105 ± 0.0159 vs 0.167 ± 0.0440 , $p=0.2232$;

and all left lobe: 0.111 ± 0.0158 vs 0.130 ± 0.1715 , $p=0.4447$) (Figure 18G). Ascorbic acid seemed to augment tissue viability in all left lung slices, but without influencing distal lung slices 24h culture.



G

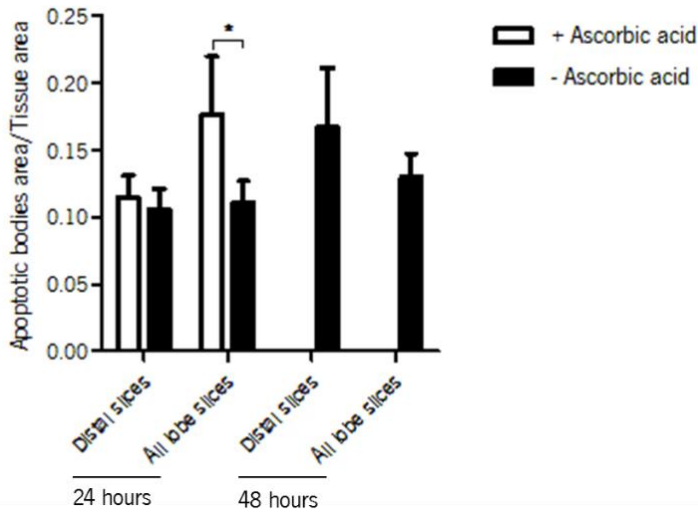


Figure 18- Different lung region slices and ascorbic acid supplementation affect tissue viability in culture.

Representative H&E staining images from lungs slices of all left lobe with (A', A'') and without (B', B'') ascorbic acid, and lungs sliced from distal area with (C', C'') and without (D', D'') ascorbic acid supplementation at 24 hours. Distal slices (E', E'') and all left lobe slice (F', F'') culture without ascorbic acid supplementation during 48 hours. (G) Tissue viability was evaluated by apoptotic bodies area quantification normalized to lung parenchyma. The photos were taken at ' 20x and '' 40x objectives. Red asterisks(*) are indicatives of apoptotic bodies. (* $p < 0.05$, ** $p < 0.01$ and *** $p < 0.0001$). Scale bars of (A'-F') images:300 μm ; (A''-F''): 50 μm .

5.DISCUSSION

5. Discussion

In the last 20 years, tissue macrophages are being considered as key regulatory agents in several organs development^{45,47,49,46,53}. However, molecular and cellular processes mediated by tissue macrophages in organ development are unknown. In lung, little is known about tissue macrophages contribution to fetal and postnatal development. In inflammation context, fetal tissue macrophages activation disrupt airways morphogenesis probably due pro-inflammatory cytokines release⁶⁰. In adult lung are known three distinct types of tissue macrophages: alveolar macrophages, interstitial macrophages and bronchial macrophages¹⁴. This classification was performed accordingly to the lung region where they are present. Alveolar macrophages are present in alveolar airspaces and are responsible for the phagocytic activity against pathogens inhaled and to maintain lung clearance through surfactant catabolism¹⁴. Interstitial macrophages are present in lung parenchyma, near to alveoli and interact with dendritic cells and interstitial lymphocytes¹⁴. Bronchial macrophages are present in lung bronchioles and were mostly involved in host-defense⁶⁸. Moreover, interstitial macrophages, have origin in the bone-marrow postnatally and under specific biological conditions^{54,69}. Other studies demonstrated that alveolar macrophages differentiate through Csf2 during postnatal period (first week after birth), also known as granulocyte/macrophage stimulating factor (Gm-csf), signaling activation^{14,57,58}. *Gm-csf*^{-/-} lungs did not present any impairments in morphology, suggesting that alveolar macrophages were not players in lung development modulation⁵⁷. Additionally, it is also described that Csf1r-positive progenitor cells came from yolk sac and present higher expression levels of F4/80⁶⁹, suggesting that interstitial macrophages arise from yolk sac and differentiate through Csf1 pathway. Recently, a work showed that during development, there are two distinct populations that arise to lung: Mac2-positive fetal macrophages and F4/80-positive embryonic macrophages⁵⁴. F4/80-positive embryonic macrophages originate “primitive” interstitial macrophages and populate lung at early stages of development (E10-12), and Mac2-positive fetal macrophages give rise to alveolar macrophages and appear latter (E14) during tissue development, both with origin from yolk sac during embryonic and fetal development, respectively, and preserved throughout adult life^{14,54}.

In the present work, we used a mice model deficient in tissue macrophages (*Csf1r*^{-/-}), promoting a disruption in macrophage differentiation via Csf1. No studies were performed to unravel tissue macrophages function during lung development using *Csf1r*^{-/-} mice model. Histological and morphometric studies measurements performed by our team in *Csf1r*^{-/-} lungs in comparison with

Csf1r^{-/-} showed a disruption in lung morphogenesis, specifically decreased airspaces area and increased non-epithelial-like volume density at saccular stage (E18.5 and P0) (Figure S2, supplementary information). Although the majority of *Csf1r*^{-/-} lungs presented severe disruption on lung, some of them were similar with *Csf1r*^{+/-} group, being designated by us as *Csf1r*^{+/-}-like. These data indicate a possible disruption on sacculation and distal epithelial differentiation due to tissue macrophages deficiency (Figure S1, supplementary information). Recently, some molecules were described as important lung modulators during fetal development, specifically in alveolar differentiation, and they present morphological defects similar to that of our *Csf1r*^{-/-} mice. Conditional knockout of histone deacetylase-3 showed impairments in alveolarization with decreased airspace areas³⁴. Full knockout of sorting nexin-5 lungs showed respiratory failure and perinatal lethality, and also decreased airspace areas⁷⁰. Therefore, we decided to evaluate alveolar epithelium differentiation state in *Csf1r*^{-/-} lungs mice, by assessment of transcript and protein expression of AT1 and AT2 cell markers. Classical AT1 markers used to assess differentiation state are *Pdpr*, *Aqp5* and *Hopx*^{31,33}. *Pdpr* is a progenitor and mature AT1 marker, but its function in lung is unknown⁷¹. *Pdpr*^{-/-} mice died at birth, and showed respiratory difficulties, and were cyanotic⁷¹. Additionally, *Pdpr*^{-/-} lungs presented increased levels of proliferation and surfactant accumulation⁷¹. Another AT1 marker studied was *Hopx* transcript expression. Loss of *Hopx* expression leads also to an increase of surfactant production accomplished with alveolar formation disruption⁷². *Aqp5* is a mature AT1 cell marker³² and it is responsible for the regulation of alveolar fluid composition³¹. *Aqp5*^{-/-} did not present impairments in lung formation³¹. However, in *Pdpr*^{-/-} lungs occurred a decrease in *Aqp5* mRNA and protein expression⁷¹. Our data showed impairments in transcript levels expression of these AT1 cell markers since canalicular stage (Figure 5-7), and protein analysis of *Aqp5* protein expression was diminished at saccular stage (E18.5 and P0) (Figure 8 and 9). These findings evidence that fetal lung tissue macrophages modulate AT1 cell differentiation.

The classical model of alveolar differentiation was based on AT2 as a source of AT1 cells³². On the other hand, disruptions in AT1 related molecules could lead to impairments in AT2 cells differentiation as seen in *Pdpr*^{-/-} and *Hopx*^{-/-} phenotypes^{71,72}. Literature was described crucial molecules involved in AT2 cellular function such as *Abca3* and surfactant proteins⁷. Absence of *Abca3* promote impairments in AT2 cellular function because disrupts lamellar bodies formation and lipid metabolism, both processes needed to a correct lung surfactant synthesis^{73,74}. *Sp-B*^{-/-} showed impairments in lamellar bodies formation and also in correctly synthesis of *Sp-A* and *Sp-C*⁷⁵. *Sp-A* and *Sp-D* are surfactant proteins associated with host defense, particularly in the

interaction between immune cells and apoptotic cells, microorganisms and virus³⁰. In our model, although AT2 transcripts and protein expression were dysregulated at E16.5 and E18.5, at P0 this phenotype was almost rescued, with similar protein expression of Sp-C. Thus, our results demonstrate that the absence of tissue macrophages leads to disturbance of alveolar differentiation, particularly in AT1 cells. However, Sp-C is also a progenitor alveolar cell marker. In this way, the question that remains is if there is a really rescue in the phenotype in *Csf1r*^{-/-} newborns or if it is occurring an accumulation of alveolar progenitor cells Sp-C positive, and consequently an impairment in AT1 cells. Sp-C co-localize with Pdpn at early stages of alveolar differentiation³³. Treutlein et al.³³ described the transcript profile of early progenitor and bipotent progenitor alveolar cells, and showed that these two progenitor populations co-express Sp-C and Pdpn³³. A way to clarify whether alveolar epithelial progenitors are being maintained in this state, and consequently AT1 and AT2 differentiation impairments, is to do an immunofluorescence using Pdpn and Sp-C and quantify the number of positive cells for both markers (early progenitor and bipotent progenitor alveolar cells).

During pseudoglandular stage, epithelium cellular fate is defined accordingly to the expression of Sox2 (proximal epithelium) and Sox9 (distal epithelium)^{17,18}. Sox9 transcript expression was also assessed in *Csf1r*^{-/-} lungs and showed a heterogenous expression pattern at E18.5 (Figure 6), but a clear increased expression at P0 (Figure 7). *Sox9* expression occurs across almost lung developmental stages, and its expression balance is a crucial factor for lung correct formation. Indeed, overexpression of *Sox9* decreased proliferation rates in distal and proximal epithelium at E14.5, and decreased expression of distal and proximal protein markers at E18.5 and P0⁷⁶. Mechanism underlying Sox9 expression regulation in lung is still unknown⁷⁶. Wnt/ β -catenin pathway was already known that it is not the signaling that regulates Sox9 expression in lung⁷⁶. Okubo et al.⁷⁷ studied N-myc function, a proto-oncogene involved in cell proliferation, differentiation, apoptosis and growth. They find out that Nmyc overexpression in lung induce Sox9 protein expression at E18.5, suggesting that Nmyc is involved in Sox9 expression regulation during lung development. Sox9 is also an important key player in ovarian and testis development in mice⁷⁸. Sox9 expression could influence the sex determination, and consequently ovarian or testis development⁷⁸. miR-124 was proposed as a candidate responsible for Sox9 regulation ovarian or testis development⁷⁸. So far, in lung it is unknown how Sox9 expression is regulated, however in tissue macrophages deficiency, Sox9 expression showed disequilibrium at E18.5 and a highly-increased expression at P0 suggesting that Sox9 balance is compromised and consequently

alveolar epithelial differentiation. Interestingly, macrophages have the capacity to synthesize and release extracellular vesicles containing mRNA or miRNA⁷⁹. Microvesicles release/absorption is a way of cellular communication. These vesicles are carriers of complex messages, including proteins, lipids, and nucleic acids and are key players in cellular communication⁸⁰. Therefore, we speculate that tissue macrophages modulate Sox9 expression through miRNA-containing extracellular vesicles release taking to Sox9 expression inhibition or other molecules involved in Sox9 expression regulation (e.g. Nmyc) and consequently alveolar epithelial differentiation.

E-cad is a classical epithelial cells marker, and it is present in lung since pseudoglandular stage with expression in pseudostratified epithelium of primitive lung buds⁸¹. At canalicular stage, E-cad is expressed in bronchial epithelial cells and followed by bronchial epithelium and primitive alveoli expression at saccular stage⁸¹. *E-cad* transcript analyses showed increased levels during canalicular stages, a clear dysregulation at E18.5 and an augment at P0 in *Csf1r*^{-/-} lung. Although morphological analyses in *Csf1r*^{-/-} lung did not showed differences in conducting airway structures, *E-cad* transcript dysregulation could indicate a proximal epithelial impairment. Moreover, in Sox9 overexpression, lungs presented decreased levels of clara and ciliated cells differentiation⁷⁶. Additionally, Nmyc overexpression lead also to Sox9 expression in saccular stage lungs, where Sox9 co-localize with Scgb1a1, a secretoglobulin highly expressed in mature clara cells⁷⁷. In fact, *Csf1r*^{-/-} lungs showed transcript dysregulation of proteins related with ciliated and neuroendocrine cells at canalicular stage (Figure 10). Besides heterogeneity expression pattern of progenitor and mature proximal epithelium related molecules at E18.5 (Figure 11), in newborn *Csf1r*^{-/-} ciliated and neuroendocrine cells maintain increased expression of their related molecules (Figure 12). Consequently, protein expression analyses should be performed in order to assess impairments in proximal epithelial cells differentiation^{76,77}.

As mentioned before, epithelium and vasculature development were two processes that occur concomitantly and interdependent during lung development. Epithelial cells release growth factors responsible for vasculature formation, such as Vegfa²⁸. Moreover, E11 lung explants cultured with Vegfa supplementation presented an increase in branching morphogenesis⁸², suggesting as a morphogen of endothelial and epithelial formation at early stages of lung development. Inhibition of Cd31 promote impairments in alveolar differentiation postnatally⁸³. Interestingly, recently it was demonstrated that this AT1 cells, the cells which differentiation was diminished in *Csf1r*^{-/-} lungs, are a Vegfa source to angiogenic alveolar development⁸⁴. Altogether, these evidences lead us to

investigate vasculature maturation during canalicular and saccular stages since it was already showed impairments in distal epithelium differentiation.

To assess vasculature maturation, we assessed transcript expression analysis of some vascular mediators involved in vasculature modulation. Fgf2 is a fibroblast growth factor involved in angiogenic development⁸⁵. Ang1 (agonist of T12 receptor), Ang2 (antagonist of T12 receptor) and Vegfa (ligand of fetal liver kinase, Flk1) are vascular mediators responsible for a correct angiogenesis process that regulate vasculature formation across lung development⁸⁶. Furthermore, endothelial progenitor cells were only Ve-cadherin-positive cells and endothelial mature cells were Ve-cadherin and Cd31-positive cells¹⁸, allowing the assessment of vasculature differentiation. Our findings showed that vasculature was affected at transcript and protein expression levels only and slightly at saccular stage (E18.5), with more severity in most of *Csf1r*^{-/-} newborns (Figures 14 to 17).

Our findings indicate that alveolar epithelium is affected by fetal tissue macrophages since canalicular stage, whereas slight vascular defects start to be observed only at saccular stage, suggesting that epithelial compartment is firstly affected by tissue macrophages absence, and consequently later vasculature formation is disturbed due to distal epithelium differentiation impairment.

One way to validate that tissue macrophages modulate alveolar differentiation during saccular stage is through inhibition of *Csf1r* *in vitro* in fetal lung slices culture at canalicular stage (E16.5). The use of this *in vitro* approach will also be very useful to investigate which regulatory pathways are being regulated by these cells (e.g. Wnt or Notch signaling). Based on published protocols^{34,65,66}, optimization of lung slices culture was performed testing two culture conditions: different lung regions slices and culture medium with ascorbic acid supplementation. Conducting airways development begins in pseudoglandular stage with neuroendocrine and ciliated cells differentiation and at canalicular stage begins secretory cell differentiation¹⁵. Distal epithelium differentiation only starts in the end of canalicular stage and occurs throughout saccular and alveolar stages until alveoli full maturation¹⁵. Different lung region slices were performed to evaluate if different regions of lung could present differential survival rates. Slices cultured of all left lobe contain bronchiole structures differentiated and immature distal epithelium. Instead, lung distal slices were performed in most distal region of left lobe, and most of the tissue were composed by immature distal epithelium. The main goal for this approach is to be able to study different epithelial sub-

compartments, since different lung regions slices could give us different inputs of information. The viability differences between all and distal lung slices were null, and supplementation with ascorbic acid increased cell death of all left lobe slices. Additionally, it was performed distal and all left lobe slices culture without ascorbic acid during 48 hours and no differences were seen in apoptotic bodies area in comparison to 24 hours of culture in the same conditions. Moreover, an observational analysis suggested that lung slices in culture for 48 hours were developing in culture with increase of airspaces and reduction of lung parenchyma thickening (data not shown). However, it is needed to increase the number of experiments in the different conditions and perform the same culture with ascorbic acid supplementation. The increase of apoptotic bodies area in all left lobe slices cultured with ascorbic acid supplementation it is not in agreement with ascorbic acid expected function. Ascorbic acid promotes oxidative protection to cells avoiding reactive oxygen species accumulation and inhibiting apoptosis mechanism activation⁶⁷. Furthermore, rodents had the capacity to synthesize ascorbic acid and its function in lung was associated to collagen synthesis⁸⁷. Geng *et al.*⁶⁵ and Wang *et al.*³⁴, on contrary of Sanford *et al.*⁶⁶, did not use ascorbic acid supplementation and culture were performed during 72 and 48 hours, respectively. So probably, ascorbic is not needed to lung slices culture in order to increase tissue viability during culture.

To conclude which of these conditions are the best to perform functional assays, more experiments should be performed to reinforce the result obtained, and other conditions tested (e.g. different culture mediums, ascorbic acid concentrations, increased time of culture). Lung morphology, alveolar differentiation, vasculature formation and apoptotic markers should be analyzed in cultured lung slices to confirm viability and development of fetal lung tissue explants in culture.

6.CONCLUSIONS

6. Conclusion and Future perspectives

The main goal for this work was to unravel tissue macrophages function during lung development, specifically during epithelium differentiation and vasculature formation. Using a tissue macrophage-deficient model, we were capable to unravel some biological processes that were affected during lung formation fetal tissue macrophages, and speculated how the processes were correlated across temporal specification. Morphological analyses showed impairments in lung formation during saccular stage (E18.5 and P0), however transcriptional analyses of epithelium showed a dysregulation in distal epithelium markers transcripts expression levels since canalicular stage. Vascular mediators' transcripts expression levels were only affected later at saccular stage, suggesting a primary alveolar epithelium compartment failure and consequently vasculature development disruption due to tissue macrophages deficiency during saccular stage. Moreover, bronchiolar epithelium markers transcripts expression was also deregulated, and protein analyses should be performed to confirm transcript phenotype dysregulation. Tissue macrophages were involved in epithelium and vasculature modulation in several organs^{45,47,49,46,53}, and in lung are involved in epithelium differentiation modulation, more specifically in alveolar epithelium differentiation. Additionally, Sox9, transcript factor responsible for distal epithelium differentiation fate⁷⁶, was clearly increased in *Csf1r*^{-/-} lungs, evidencing that absence of tissue macrophages leads to Sox9 overexpression in *Csf1r*^{-/-} at saccular stage, suggesting an interruption on progenitor distal epithelial cells fate. In this way, results from this work suggest that tissue macrophages could be key mediators, probably by release of regulatory factors, as soluble factors and miRNA, in Sox9 expression regulation during lung development.

In the future, Sox9 protein expression across lung development should be analyzed to confirm progenitor cells accumulation and/or dysregulations in proximal-distal epithelium transition. Moreover, bioinformatic analyses should be performed to indicate potential miRNA Sox9-target and perform functional assays using lungs slices cultures to answer whether that predicted miRNA is the Sox9 regulatory mechanism mediated by tissue macrophages.

7.REFERENCES

7. References

1. Pike, K. C. & Lucas, J. S. A. Respiratory consequences of late preterm birth. *Paediatric Respiratory Reviews* **16**, 182–188 (2015).
2. Warburton, D. *et al.* Lung organogenesis. *Curr. Top. Dev. Biol.* **90**, 73–158 (2010).
3. Bourbon, J., Boucherat, O., Chailley-Heu, B. & Delacourt, C. Control Mechanisms of Lung Alveolar Development and Their Disorders in Bronchopulmonary Dysplasia. *Pediatric Research* **57**, 38R–46R (2005).
4. Patel, R. M. *et al.* Causes and Timing of Death in Extremely Premature Infants from 2000 through 2011. *N. Engl. J. Med.* **372**, 331–340 (2015).
5. Corroyer, S., Schittny, J. C., Djonov, V. & Burri, P. H. Impairment of Rat Postnatal Lung Alveolar Development by Glucocorticoids : Involvement of Kinase Inhibitors. *Pediatr. Res.* **51**, 169–176 (2002).
6. Reynolds, R. M. Glucocorticoid excess and the developmental origins of disease: Two decades of testing the hypothesis - 2012 Curt Richter Award Winner. *Psychoneuroendocrinology* **38**, 1–11 (2013).
7. Rock, J. R. & Hogan, B. L. M. Epithelial progenitor cells in lung development, maintenance, repair, and disease. *Annu. Rev. Cell Dev. Biol.* **27**, 493–512 (2011).
8. Rokicki, W., Rokicki, M., Wojtacha, J. & Dzeljijli, A. The role and importance of club cells (Clara cells) in the pathogenesis of some respiratory diseases. *Kardiochirurgia i Torakochirurgia Pol.* **13**, 26–30 (2016).
9. Linnoila, R. I. Functional facets of the pulmonary neuroendocrine system. *Lab. Invest.* **86**, 425–44 (2006).
10. Branchfield, K. *et al.* Pulmonary neuroendocrine cells function as airway sensors to control lung immune response. *Science* **351**, 707–710 (2016).
11. Barron, L., Gharib, S. A. & Duffield, J. S. Lung Pericytes and Resident Fibroblasts: Busy Multitaskers. *American Journal of Pathology* **186**, 2519–2531 (2016).
12. Schittny, J. C. Development of the lung. *Cell and Tissue Research* **367**, 427–444 (2017).

13. Bergers, G. The role of pericytes in blood-vessel formation and maintenance. *Neuro. Oncol.* **7**, 452–464 (2005).
14. Kopf, M., Schneider, C. & Nobs, S. P. The development and function of lung-resident macrophages and dendritic cells. *Nat Immunol* **16**, 36–44 (2015).
15. Rackley, C. R. & Stripp, B. R. Building and maintaining the epithelium of the lung. *Journal of Clinical Investigation* **122**, 2724–2730 (2012).
16. Maeda, Y., Davé, V. & Whitsett, J. a. Transcriptional control of lung morphogenesis. *Physiol. Rev.* **87**, 219–44 (2007).
17. Morrisey, E. E. & Hogan, B. L. M. Preparing for the First Breath: Genetic and Cellular Mechanisms in Lung Development. *Developmental Cell* **18**, 8–23 (2010).
18. Herriges, M. & Morrisey, E. E. Lung development: orchestrating the generation and regeneration of a complex organ. *Development* **141**, 502–513 (2014).
19. deMello, D. E., Sawyer, D., Galvin, N. & Reid, L. M. Early fetal development of lung vasculature. *Am J Respir Cell Mol Biol* **16**, 568–81. (1997).
20. Hall, S. M., Hislop, A. A., Pierce, C. M. & Haworth, S. G. Prenatal origins of human intrapulmonary arteries formation and smooth muscle maturation. *Am. J. Respir. Cell Mol. Biol.* **23**, 194–203 (2000).
21. Parera, M. C. *et al.* Distal angiogenesis: a new concept for lung vascular morphogenesis. *Am. J. Physiol. Lung Cell. Mol. Physiol.* **288**, L141–L149 (2005).
22. Peng, T. *et al.* Coordination of heart and lung co-development by a multipotent cardiopulmonary progenitor. *Nature* **500**, 589–592 (2013).
23. Metzger, R. J., Klein, O. D., Martin, G. R. & Krasnow, M. A. The branching programme of mouse lung development. *Nature* **453**, 745–750 (2008).
24. Chuang, P.-T. & McMahon, A. P. Branching morphogenesis of the lung: new molecular insights into an old problem. *Trends Cell Biol.* **13**, 86–91 (2016).
25. Zhao, L., Wang, K., Ferrara, N. & Vu, T. H. Vascular endothelial growth factor co-ordinates proper development of lung epithelium and vasculature. *Mech. Dev.* **122**, 877–886 (2005).

26. White, A. C. *et al.* FGF9 and SHH signaling coordinate lung growth and development through regulation of distinct mesenchymal domains. *Development* **133**, 1507–1517 (2006).
27. Lazarus, A. *et al.* A perfusion-independent role of blood vessels in determining branching stereotypy of lung airways. *Development* **138**, 2359–2368 (2011).
28. Akeson, A. L. *et al.* Temporal and spatial regulation of VEGF-A controls vascular patterning in the embryonic lung. *Dev. Biol.* **264**, 443–455 (2003).
29. Whitsett, J. A., Wert, S. E. & Weaver, T. E. Alveolar surfactant homeostasis and the pathogenesis of pulmonary disease. *Annu. Rev. Med.* **61**, 105–19 (2010).
30. Wright, J. R. Immunoregulatory functions of surfactant proteins. *Nat. Rev. Immunol.* **5**, 58–68 (2005).
31. Williams, M. C. Alveolar type I cells: molecular phenotype and development. *Annu. Rev. Physiol.* **65**, 669–95 (2003).
32. Desai, T. J., Brownfield, D. G. & Krasnow, M. A. Alveolar progenitor and stem cells in lung development, renewal and cancer. *Nature* **507**, 190–194 (2014).
33. Treutlein, B. *et al.* Reconstructing lineage hierarchies of the distal lung epithelium using single-cell RNA-seq. *Nature* **509**, 371–5 (2014).
34. Wang, Y. *et al.* HDAC3-Dependent Epigenetic Pathway Controls Lung Alveolar Epithelial Cell Remodeling and Article HDAC3-Dependent Epigenetic Pathway Controls Lung Alveolar Epithelial Cell Remodeling and Spreading via miR-17-92 and TGF- β Signaling Regulation. *Dev. Cell* **36**, 303–315 (2016).
35. Loscertales, M. *et al.* Type IV collagen drives alveolar epithelial–endothelial association and the morphogenetic movements of septation. *BMC Biol.* **14**, 59 (2016).
36. Tsao, P.-N. *et al.* Epithelial Notch signaling regulates lung alveolar morphogenesis and airway epithelial integrity. *Proc. Natl. Acad. Sci.* **113**, 8242–8247 (2016).
37. Frank, D. B. *et al.* Emergence of a Wave of Wnt Signaling that Regulates Lung Alveologenesis by Controlling Epithelial Self-Renewal and Differentiation. *Cell Rep.* **17**, 2312–2325 (2016).

38. Chelly, N., Mouhieddine-Gueddiche, O. B., Barlier-Mur, a M., Chailley-Heu, B. & Bourbon, J. R. Keratinocyte growth factor enhances maturation of fetal rat lung type II cells. *Am. J. Respir. Cell Mol. Biol.* **20**, 423–32 (1999).
39. Lee, C. S., Sund, N. J., Behr, R., Herrera, P. L. & Kaestner, K. H. Foxa2 is required for the differentiation of pancreatic α cells. *Dev. Biol.* **278**, 484–495 (2005).
40. Gautier, E. L. *et al.* Gene expression profiles and transcriptional regulatory pathways underlying mouse tissue macrophage identity and diversity. *Nat. Immunol.* **13**, 1118–1128 (2012).
41. Wynn, T. A., Chawla, A. & Pollard, J. W. Macrophage biology in development, homeostasis and disease. *Nature* **496**, 445–55 (2013).
42. Mass, E. *et al.* Specification of tissue-resident macrophages during organogenesis. *Science* **353**, 1892–1904 (2016).
43. Jones, C. V & Ricardo, S. D. Macrophages and CSF-1: implications for development and beyond. *Organogenesis* **9**, 249–60 (2013).
44. Pixley, F. J. & Stanley, E. R. CSF-1 regulation of the wandering macrophage: Complexity in action. *Trends in Cell Biology* **14**, 628–638 (2004).
45. Rae, F. *et al.* Characterisation and trophic functions of murine embryonic macrophages based upon the use of a Csf1r-EGFP transgene reporter. *Dev. Biol.* **308**, 232–246 (2007).
46. Fantin, A. *et al.* Tissue macrophages act as cellular chaperones for vascular anastomosis downstream of VEGF-mediated endothelial tip cell induction. *Blood* **116**, 829–840 (2010).
47. Geutskens, S. B., Otonkoski, T., Pulkkinen, M., Drexhage, H. a & Leenen, P. J. M. Macrophages in the murine pancreas and their involvement in fetal endocrine development in vitro. *J. Leukoc. Biol.* **78**, 845–52 (2005).
48. Banaei-Bouchareb, L. *et al.* Insulin cell mass is altered in Csf1op/Csf1op macrophage-deficient mice. *J. Leukoc. Biol.* **76**, 359–67 (2004).
49. Gouon-Evans, V., Rothenberg, M. E. & Pollard, J. W. Postnatal mammary gland

- development requires macrophages and eosinophils. *Development* **127**, 2269–82 (2000).
50. Erlich, B., Zhu, L., Etgen, A. M., Dobrenis, K. & Pollard, J. W. Absence of colony stimulation factor-1 receptor results in loss of microglia, disrupted brain development and olfactory deficits. *PLoS One* **6**, (2011).
 51. Pollard, J. W. Trophic macrophages in development and disease. *Nat. Rev. Immunol.* **9**, 259–270 (2009).
 52. Dai, X. M. *et al.* Targeted disruption of the mouse colony-stimulating factor 1 receptor gene results in osteopetrosis, mononuclear phagocyte deficiency, increased primitive progenitor cell frequencies, and reproductive defects. *Blood* **99**, 111–120 (2002).
 53. Vi, L. *et al.* Macrophages promote osteoblastic differentiation in-vivo: Implications in fracture repair and bone homeostasis. *J. Bone Miner. Res.* **30**, 1090–1102 (2015).
 54. Tan, S. Y. S. & Krasnow, M. A. Developmental origin of lung macrophage diversity. *Development* **143**, 1318–1327 (2016).
 55. Rosenberg, I., Cherayil, B. J., Isselbacher, K. J. & Pillai, S. Mac-2-binding glycoproteins: Putative ligands for a cytosolic beta-galactoside lectin. *J. Biol. Chem.* **266**, 18731–18736 (1991).
 56. Lin, H. H., Stacey, M., Stein-Streilein, J. & Gordon, S. F4/80: The macrophage-specific adhesion-GPCR and its role in immunoregulation. *Adv. Exp. Med. Biol.* **706**, 149–156 (2010).
 57. Stanley, E. *et al.* Granulocyte/macrophage colony-stimulating factor-deficient mice show no major perturbation of hematopoiesis but develop a characteristic pulmonary pathology. *Med. Sci.* **91**, 5592–55 (1994).
 58. Guilliams, M. *et al.* Alveolar macrophages develop from fetal monocytes that differentiate into long-lived cells in the first week of life via GM-CSF. *J. Exp. Med.* **210**, 1977–1992 (2013).
 59. Nogueira-Silva, C., Santos, M., Baptista, M. J., Moura, R. S. & Correia-Pinto, J. IL-6 is constitutively expressed during lung morphogenesis and enhances fetal lung explant branching. *Pediatr. Res.* **60**, 530–536 (2006).

60. Blackwell, T. S. *et al.* NF- κ B Signaling in Fetal Lung Macrophages Disrupts Airway Morphogenesis. *J. Immunol.* **187**, 2740–2747 (2011).
61. Livak, K. J. & Schmittgen, T. D. Analysis of relative gene expression data using real-time quantitative PCR and the 2^{(-Delta Delta C(T))} Method. *Methods* **25**, 402–8 (2001).
62. Sumedha, S., Kotrashetti, V., Somannavar, P., Nayak, R. & Babji, D. A histochemical comparison of methyl green-pyronin, and hematoxylin and eosin for detecting apoptotic cells in oral squamous cell carcinoma, oral leukoplakia, oral submucous fibrosis and normal oral mucosa. *Biotech. Histochem.* **90**, 264–269 (2015).
63. Mariotto, A., Pavlova, O., Park, H. S., Huber, M. & Hohl, D. HOPX: The Unusual Homeodomain-Containing Protein. *Journal of Investigative Dermatology* **136**, 905–911 (2016).
64. Jain, R. *et al.* Plasticity of Hopx(+) type I alveolar cells to regenerate type II cells in the lung. *Nat. Commun.* **6**, 6727 (2015).
65. Geng, Y. *et al.* Follistatin-like 1 (Fstl1) is a bone morphogenetic protein (BMP) 4 signaling antagonist in controlling mouse lung development. *Proc. Natl. Acad. Sci.* **108**, 7058–7063 (2011).
66. Sanford, E. L. *et al.* MiR-449a affects epithelial proliferation during the pseudoglandular and canalicular phases of avian and mammal lung development. *PLoS One* **11**, (2016).
67. Padh, H. Cellular functions of ascorbic acid. *Biochem. Cell Biol.* **68**, 1166–1173 (1990).
68. Balhara, J. & Gounni, a S. The alveolar macrophages in asthma: a double-edged sword. *Mucosal Immunol.* **5**, 605–9 (2012).
69. Gomez Perdiguero, E. *et al.* Tissue-resident macrophages originate from yolk-sac-derived erythro-myeloid progenitors. *Nature* **518**, 547–551 (2014).
70. Im, S. K. *et al.* Disruption of Sorting Nexin 5 Causes Respiratory Failure Associated with Undifferentiated Alveolar Epithelial Type I Cells in Mice. *PLoS One* **8**, (2013).
71. Ramirez, M. I. *et al.* T1alpha, a lung type I cell differentiation gene, is required for normal lung cell proliferation and alveolus formation at birth. *Developmental Biology* **256**, 61–72 (2003).

72. Yin, Z. *et al.* Hop functions downstream of Nkx2.1 and GATA6 to mediate HDAC-dependent negative regulation of pulmonary gene expression. *Am J Physiol Lung Cell Mol Physiol* **291**, L191-9 (2006).
73. Ban, N. *et al.* ABCA3 as a lipid transporter in pulmonary surfactant biogenesis. *J. Biol. Chem.* **282**, 9628–9634 (2007).
74. Fitzgerald, M. L. *et al.* ABCA3 inactivation in mice causes respiratory failure, loss of pulmonary surfactant, and depletion of lung phosphatidylglycerol. *J. Lipid Res.* **48**, 621–32 (2007).
75. Clark, J. C. *et al.* Targeted disruption of the surfactant protein B gene disrupts surfactant homeostasis, causing respiratory failure in newborn mice. *Cell Biol.* **92**, 7794–7798 (1995).
76. Rockich, B. E. *et al.* Sox9 plays multiple roles in the lung epithelium during branching morphogenesis. *Proc. Natl. Acad. Sci. U. S. A.* **110**, E4456-64 (2013).
77. Okubo, T., Knoepfler, P. S., Eisenman, R. N. & Hogan, B. L. Nmyc plays an essential role during lung development as a dosage-sensitive regulator of progenitor cell proliferation and differentiation. *Development* **132**, 1363–1374 (2005).
78. Real, F. M. *et al.* A microRNA (mmu-miR-124) prevents Sox9 expression in developing mouse ovarian cells. *Biol. Reprod.* **89**, 78 (2013).
79. Ismail, N. *et al.* Macrophage microvesicles induce macrophage differentiation and miR-223 transfer. *Blood* **121**, 984–995 (2013).
80. Maas, S. L. N., Breakefield, X. O. & Weaver, A. M. Extracellular Vesicles: Unique Intercellular Delivery Vehicles. *Trends in Cell Biology* **27**, 172–188 (2017).
81. Kasper, M., Behrens, J., Schuh, D. & Müller, M. Distribution of E-cadherin and Ep-CAM in the human lung during development and after injury. *Histochem. Cell Biol.* **103**, 281–6 (1995).
82. Moral, P. Del & Keshet, E. VEGF-A signaling through Flk-1 is a critical facilitator of early embryonic lung epithelial to endothelial crosstalk and branching morphogenesis. **290**, 177–188 (2006).

83. DeLisser, H. M. *et al.* Loss of PECAM-1 function impairs alveolarization. *J. Biol. Chem.* **281**, 8724–8731 (2006).
84. Yang, J. *et al.* Development and Plasticity of Alveolar type 1 Cells. *Development* **143**, 54–65 (2015).
85. Slavin, J. Fibroblast growth factors: at the heart of angiogenesis. *Cell biology international* **19**, 431–44 (1995).
86. Hanahan, D., Mikawa, T. & Bader, D. M. Signaling vascular morphogenesis and maintenance. *Science* **277**, 48–50 (1997).
87. Koike, K. *et al.* Complete lack of vitamin C intake generates pulmonary emphysema in senescence marker protein-30 knockout mice. *Am. J. Physiol. Cell. Mol. Physiol.* **298**, 784–792 (2010).
88. Sun, S., Schiller, J. H. & Gazdar, A. F. Lung cancer in never smokers – a different disease. *Nat. Rev. Cancer* **7**, 778–790 (2007).

8.SUPPLEMENTARY INFORMATION

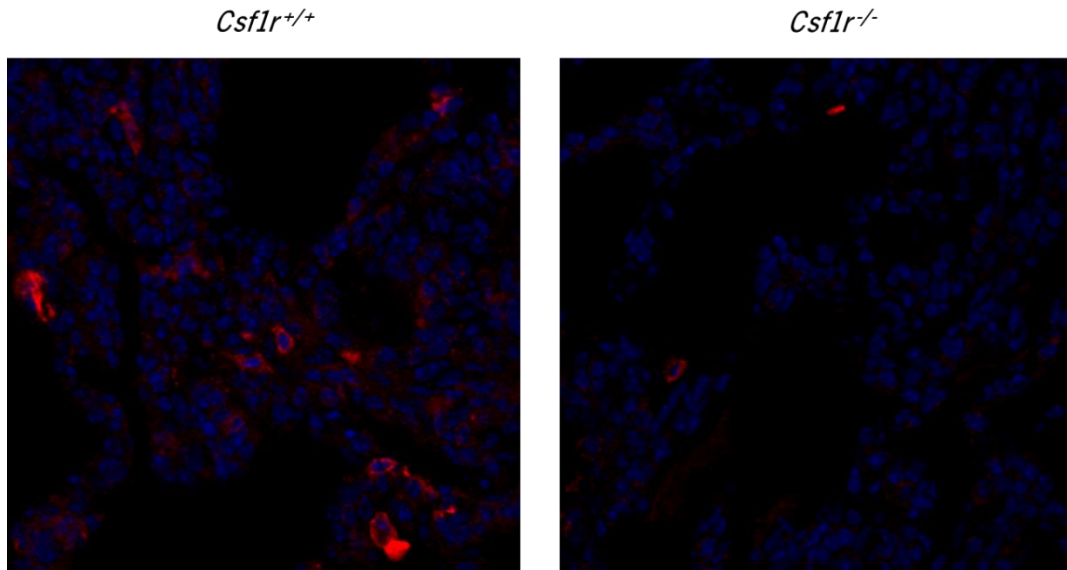


Figure S1- Drastic reduction of tissue macrophages in *Csf1r*^{-/-} lungs.

F4/80 protein expression was evaluated by immunofluorescence and F4/80+ cells counted. F4/80 positive cells were more than 85% decrease in *Csf1r*^{-/-} lungs.

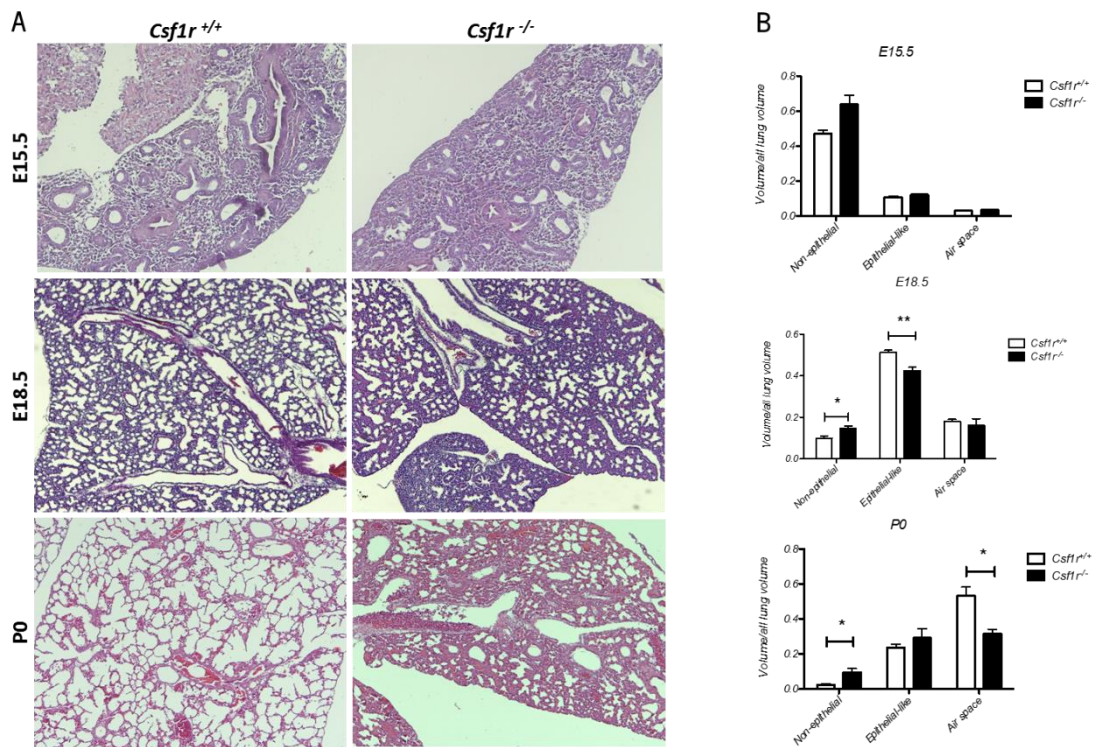


Figure S2- Tissue macrophages disrupt lung morphology at fetal and post-natal saccular stage.

(A) Histological lungs sections stained H&E at E15.5, E18.5 and P0 of *Csf1r*^{-/-} and *Csf1r*^{+/+} mice. (B) Stereological analysis of lung morphology. Mesenchyme-like, epithelial-like and air space volume densities (VD) were measured in glutaraldehyde-fixed and methacrylate-embedded tissues. N= 4-6 mice per group from at least 3 independent litters.